Cancer Chemother Pharmacol (2010) 65:243–250
DOI 10.1007/s00280-009-1028-3

ORIGINAL ARTICLE

Phase I clinical and pharmacokinetic study of the glucose-conjugated cytotoxic agent D-19575 (glufosfamide) in patients with solid tumors

Toshio Shimizu · Isamu Okamoto · Kenji Tamura · Taroh Satoh · Masaki Miyazaki · Yusaku Akashi · Tomohiro Ozaki · Masahiro Fukuoka · Kazuhiko Nakagawa

Received: 20 January 2009 / Accepted: 4 May 2009 / Published online: 29 May 2009

Abstract
Purpose D-19575 (glufosfamide: β-D-glucosylisophosphoramide mustard) is an alkylating agent in which isophosphoramide mustard, the cytotoxic metabolite of ifosfamide, is covalently linked to β-D-glucose. We have performed a phase I study to determine the safety profile, pharmacokinetics, and antitumor activity of D-19575 in Japanese patients with advanced solid tumors
Methods Patients were treated with escalating doses of D-19575 administered by a two-step (fast–slow) intravenous infusion over 6 h every 3 weeks. Thirteen patients received 43 treatment cycles (median 3; range 1–11) at D-19575 doses of 3,200, 4,500, or 6,000 mg/m^2.
Results Hematologic toxicities and other side effects were generally mild. The maximum tolerated dose of D-19575 was 6,000 mg/m^2, at which two patients experienced dose-limiting toxicities (hypophosphatemia, hypokalemia, and metabolic acidosis each of grade 3). Pharmacokinetic analysis revealed a linear relation between the area under the concentration-versus-time curve (AUC) and dose. The AUC values for isophosphoramide mustard were substantially greater than those achieved by bolus administration or continuous infusion of ifosfamide in conventional therapy. One patient with gallbladder cancer previously treated with cisplatin and gemcitabine achieved a partial response lasting for >5 months, and eight patients achieved disease stabilization.
Conclusions Our results show that D-19575 can be safely administered by infusion over 6 h at 4,500 mg/m^2 every 3 weeks. The safety profile and potential antitumor activity of D-19575 show that phase II studies of this drug are warranted.

Keywords Glufosfamide · Isophosphoramide mustard · Glucose transporter · Pharmacokinetics

T. Shimizu · I. Okamoto (✉) · T. Satoh · M. Miyazaki · K. Nakagawa
Department of Medical Oncology,
Kinki University School of Medicine, 377-2 Ohno-higashi,
Osaka-Sayama, Osaka 589-8511, Japan
e-mail: chi-okamoto@dotd.med.kindai.ac.jp

K. Tamura
Outpatient Treatment Center, National Cancer Center Hospital,
5-1-1 Tsukiji, Chuo-ku, Tokyo 104-0045, Japan

Y. Akashi · T. Ozaki
Department of Medical Oncology,
Kinki University Nara Hospital, 1248-1 Otoda-cho,
Ikoma, Nara 630-0293, Japan

M. Fukuoka
Department of Medical Oncology,
Kinki University Sakai Hospital, 2-7-1 Harayamadai,
Minami-ku Sakai, Osaka 590-0132, Japan

Introduction

D-19575 (glufosfamide: β-D-glucosylisophosphoramide mustard) is a new-generation cytotoxic alkylating agent in which isophosphoramide mustard (IPM), the active metabolite of ifosfamide (IFO), is covalently linked to β-D-glucose (Fig. 1). The structure and metabolism of the D-19575 molecule are thought to be associated with two therapeutic advantages: a reduced generation of toxic metabolites compared with IFO, and targeting by the glucose moiety to rapidly proliferating tumor cells [1, 2].

Rapidly proliferating and energy-consuming cancer cells have been shown to overexpress certain glucose transporter proteins [3, 4]. D-19575 has the potential to target tumor

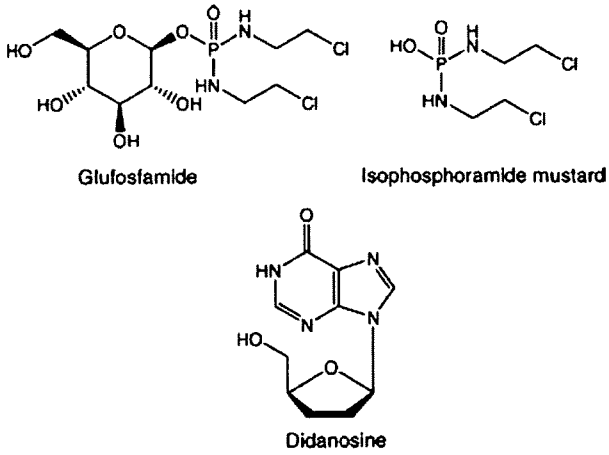

Fig. 1 Structures of D-19575 (glufosfamide), isophosphoramide mustard (the active cytotoxic metabolite of D-19575), and didanosine (internal standard)

cells by serving as a substrate for such glucose transporters in the plasma membrane [5–7]. Together with the increased metabolic rate and glucose consumption of tumor cells, this targeting mechanism may contribute to the relative selectivity of D-19575 for tumor cells.

Another characteristic of D-19575 is that, because of the absence of the oxazophosphorine ring in its structure, it does not release the urothelium irritant acrolein, which has been shown to induce hemorrhagic cystitis in individuals treated with IFO [2]. Moreover, the amount of toxic chloroacetaldehyde generated metabolically after administration of D-19575 is markedly reduced compared with that generated after IFO administration (unpublished data). Although the pathogenesis of IFO-induced nephrotoxicity is poorly understood, the reduced production of chloroacetaldehyde may minimize such toxicity of D-19575. Preclinical pharmacokinetic analysis of D-19575 has revealed that the drug is rapidly cleared by the kidneys and has favorable tissue-distribution and protein-binding profiles [8]. Toxicity studies in rodents have shown that D-19575 is more toxic when administered orally than intravenously, apparently because of a pronounced first-pass effect and increased production of toxic metabolites (data on file; ASTA Medica AG, Germany).

The aims of the present study were to determine the maximum tolerated dose (MTD) and dose-limiting toxicities (DLTs) of D-19575, to otherwise evaluate the safety profile of the drug, and to analyze its pharmacokinetics after administration by biphasic (fast–slow) intravenous infusion over 6 h every 3 weeks in Japanese patients with refractory advanced solid tumors. Furthermore, we performed a pharmacokinetic analysis of IPM generated from D-19575.

Patients and methods

Study objectives

This phase I study aimed to evaluate the safety (including DLTs and MTD) and pharmacokinetic profiles of D-19575 administered by intravenous infusion over 6 h in Japanese individuals with solid tumors who relapsed after adequate or standard chemotherapy or in those with advanced or metastatic solid tumors for whom no effective standard therapy was available. The study was fully supported by Medibic Pharma Co. Ltd (Tokyo, Japan) as a registration-directed clinical trial. D-19575 was synthesized in the Chemical Research Laboratories of ASTA Medica AG (Frankfurt, Germany). ASTA Medica AG's oncology division was acquired by Baxter International in 2001, but Baxter International itself terminated D-19575 development and shortly thereafter licensed their rights to Threshold Pharmaceuticals (Redwood City, CA, USA). In this study, D-19575 was supplied by Medibic Pharma Co. Ltd. Medibic Pharma and Threshold Pharmaceuticals agreed to co-develop D-19575 in Asia on December 2004.

Eligibility

Eligible patients were individuals aged 20–75 years who had solid tumors that were either refractory to conventional treatment or for which no standard treatment was available; had an Eastern Cooperative Oncology Group (ECOG) performance status of 0 or 1; had adequate hematopoietic reserves [absolute neutrophil count (ANC) of $\geq$1,500/μL, platelet count of $\geq$100,000/μL, hemoglobin concentration of $\geq$9.0 g/dL]; had serum total bilirubin and creatinine concentrations of $\leq$1.5 times the upper limit of institutional normal (ULN); had serum aspartate aminotransferase and alanine aminotransferase activities of $\leq$2.5 times ULN; had not received chemotherapy or radiation therapy within the previous 4 weeks; had no exposure to nitrosoureas or mitomycin within the previous 6 weeks; and had given consent to be hospitalized during the first course of treatment with D-19575. Patients were ineligible if they had symptomatic brain metastasis; other nonmalignant systemic disease; an active, uncontrolled infection; preexisting nephrotoxicity of grade 3 or 4 [National Cancer Institute Common Toxicity Criteria (NCI-CTC)] resulting from previous therapy; or infection with human immunodeficiency virus or hepatitis B or C virus. They were also ineligible if they were pregnant or nursing, or if they required steroid therapy. All patients provided written informed consent before entering the study. The study was approved by the Institutional Review Board at each participating center and conducted in accordance with the Declaration of Helsinki and good clinical practice guidelines.

A medical history was obtained from each patient, and physical examinations and routine laboratory evaluations were performed before treatment initiation and weekly thereafter. Chest and other relevant X-rays were obtained during screening and after alternate cycles of treatment. Adverse events were monitored and recorded throughout the study and were graded according to NCI-CTC, version 3.0. The tumor response was assessed for measurable target lesions according to Response Evaluation Criteria in Solid Tumors (RECIST).

Treatment administration

This open-label, dose-escalation phase I study of D-19575 was based on intravenous infusion of the drug in three cohorts of Japanese subjects with malignant solid tumors. D-19575 was administered intravenously over 6 h in a total volume of 1,000 mL of normal saline at doses of 3,200, 4,500, and 6,000 mg/m^2. One-quarter of the dose was administered during the first 30 min at a rate of 500 mL/h, with the remainder of the dose being administered over the subsequent 330 min at a rate of 136 mL/h. D-19575 was administered on day 1 once every 3 weeks. Antiemetic premedication was not mandatory in the protocol. Granulocyte colony-stimulating factor (G-CSF) was administered for febrile neutropenia, sepsis with neutropenia, or recurrent neutropenia of grade 4.

DLTs and MTD

The starting dose of D-19575 was 3,200 mg/m^2, which was increased to 4,500 and then to 6,000 mg/m^2 in subsequent cohorts of at least three patients. The following adverse events during cycle 1 were defined as DLTs: neutropenia of grade 4 (ANC of <500/μL) for >7 days; febrile neutropenia (fever of >38.0°C with an ANC of <1,000/μL); thrombocytopenia (platelet count of <25,000/μL); nausea or vomiting of grade ≥3 despite maximal antiemetic therapy; and any other nonhematologic toxicity of grade ≥3 considered related to D-19575. If any patient experienced a DLT during the first cycle, three additional patients were treated at the same dose. Patients who experienced a DLT could continue D-19575 therapy at the preceding dose level. Treatment in subsequent courses was reinitiated only after hematologic recovery (ANC of ≥1,500/μL, platelet count of ≥100,000/μL) and resolution of all other toxicities to grade ≤1 or baseline intensity. The MTD was defined as the dose at which two or more patients experienced a DLT in the first cycle. The recommended dose was defined as the dose level immediately below the MTD.

Pharmacokinetic analysis

Pharmacokinetic sampling was performed for the first and second cycles. Blood samples (2.0 mL) for analysis of the plasma concentrations of D-19575 and IPM were collected at 10 time points on the day of drug administration (total volume of 20 mL of blood): immediately before the start of drug infusion and at 0.5, 1, 3, 6 (immediately before the end of infusion), 6.5, 7, 8, 12, and 24 h after the start of infusion. Plasma samples were stored at –70°C until analysis. D-19575 and IPM in plasma samples were measured by high-performance liquid chromatography and tandem mass spectrometry at Covance Bioanalytical Services (Indianapolis, IN, USA).

The plasma concentration-versus-time data for D-19575 and IPM in cycles 1 and 2 were analyzed with a noncompartmental method. The pharmacokinetic parameters of D-19575 and IPM determined included the maximum observed plasma concentration (C_{max}), time to reach C_{max} (T_{max}), area under the plasma concentration–time curve from time zero to infinity ($AUC_{0-\infty}$), terminal elimination half-time ($t_{1/2}$), total body clearance (CL_{tot}), and volume of distribution at steady state (V_{ss}). The $AUC_{0-\infty}$ was determined by summing the area from time zero to the time of the last measured concentration (as calculated with the use of a log trapezoidal method) and the extrapolated area. The extrapolated area was determined by dividing the final concentration by the slope (k) of the terminal log linear phase. The absolute value of k was also used to estimate the apparent terminal elimination half-time: $t_{1/2} = \ln(2/k)$. The CL_{tot} was determined by dividing dose by $AUC_{0-\infty}$. The V_{ss} was calculated by multiplying CL_{tot} by the mean residence time, which was determined as the area under the moment curve to infinity divided by $AUC_{0-\infty}$. All pharmacokinetic parameters were calculated with the use of WinNonlin Professional 5.0 software (Pharsight Corporation, Mountain View, CA, USA), and all calculations were performed with the actual times recorded on the case report form and with zero substituted for concentrations below the quantification limit of the assay (5 ng/mL for both D-19575 and IPM). The plasma concentrations of D-19575 and IPM (day 1 of cycles 1 and 2) were listed by subject and summarized by dose (mean, standard deviation, coefficient of variation, minimum, maximum, number of observations). Dose-adjusted $AUC_{0-\infty}$ and C_{max} values were calculated for each subject by dividing $AUC_{0-\infty}$ and C_{max} by dose. Analysis of variance appropriate for a parallel, dose-ascending design was performed on the dose-adjusted parameters to assess dose proportionality. Individual and mean plasma concentrations of D-19575 and IPM versus time after administration of D-19575 were tabulated and presented graphically on both linear and logarithm scales. For the time course graphs,

values below the quantification limit of the assay were set to zero.

Results

Patient characteristics

Thirteen patients (nine men and four women; median age, 62 years) were enrolled in the study between January and August 2007. Patient characteristics are shown in Table 1. Most patients were heavily pretreated, with the median number of prior chemotherapy regimens being three.

Table 1 Patient characteristics

Characteristic	No. of patients (n = 13)
Sex (male/female)	9/4
Age (years)	
Median	62
Range	51–73
ECOG performance status	
0	3
1	10
Tumor type	
Colorectal cancer	7
Non-small cell lung cancer	1
Thymic cancer	1
Thymoma	1
Gallbladder cancer	1
Gastric cancer	1
Uterine corpus-endometrial cancer	1
Previous treatment	
Chemotherapy (no. of regimens)	
1	1
2	4
3	3
4	1
≥5	4
Radiation	3
Surgery	12

DLTs and MTD

Patient distribution by dose level is shown in Table 2. No DLTs occurred in the patient cohorts treated with D-19575 at the doses of 3,200 mg/m^2 (n = 3) or 4,500 mg/m^2 (n = 7). At the dose of 6,000 mg/m^2, however, two of three treated patients experienced DLTs: One patient experienced metabolic acidosis and hypophosphatemia of grade 3, the other patient experienced hypophosphatemia and hypokalemia of grade 3. All DLTs were transient and reversible. The dose of 6,000 mg/m^2 was thus identified as the MTD, and enrollment of patients in the study was stopped. The recommended dose level for phase II evaluation was therefore determined to be 4,500 mg/m^2.

Safety

A total of 43 cycles of treatment was administered to the 13 patients, with a median of three cycles per patient and a range of 1–11 (Table 2). The incidence of hematologic toxicities by dose level is shown in Table 3. Clinically significant effects on ANC or platelet count were rare and only one patient, treated at the dose of 4,500 mg/m^2, experienced neutropenia of grade 4 without infection, which occurred during cycle 2 and was short-lived. Red blood cell transfusion was required in one patient treated at the dose of 4,500 mg/m^2 during cycle 3 because of the development of grade 4 anemia. Other hematologic toxicities were mostly of grade 1 or 2 and were reversible. The predominant nonhematologic toxicities were fatigue, nausea, a high urinary concentration of β_2-microglobulin, hypophosphatemia, hypokalemia, and metabolic acidosis (Table 4). Nonhematologic toxicities were also generally transient and reversible.

Pharmacokinetics

Plasma samples were obtained from all 13 patients during the first and second cycles of treatment. Plots of the mean plasma concentrations of D-19575 and IPM (the active metabolite of D-19575) versus time are shown in Fig. 2a. There was substantial interpatient variability in the pharmacokinetics of D-19575 after intravenous administration

Table 2 Dose-escalation scheme and summary of DLT incidence

Dose (mg/m^2)	No. of patients	No. of cycles	No. of patients with DLT	DLT (grade)
3,200	3	8	0	
4,500	7	28	0	
6,000	3	7	2	Hypophosphatemia (grade 3), hypokalemia (grade 3), metabolic acidosis (grade 3)
Total	13	43	2	

Table 3 No. of patients with hematologic toxicities (all cycles)

Dose (mg/m^2)	No. of patients	Neutropenia				Anemia				Thrombocytopenia			
		Grade 1	Grade 2	Grade 3	Grade 4	Grade 1	Grade 2	Grade 3	Grade 4	Grade 1	Grade 2	Grade 3	Grade 4
3,200	3	1	0	1	0	1	0	0	0	0	0	0	0
4,500	7	1	0	1	1	2	1	0	1	2	0	1	0
6,000	3	0	1	0	0	0	0	0	0	1	0	0	0
Total	13	2	1	2	1	3	1	0	1	3	0	1	0

Table 4 Number of patients with nonhematologic toxicities (all cycles)

Dose (mg/m^2)	No. of patients	Fatigue/generalized weakness				Hypophosphatemia				Hypokalemia				Metabolic acidosis			
		Grade				Grade				Grade				Grade			
		1	2	3	4	1	2	3	4	1	2	3	4	1	2	3	4
3,200	3	3	0	0	0	0	1	0	0	0	0	0	0	1	0	1	0
4,500	7	6	2	0	0	0	2	2	0	1	0	1	1	0	0	2	0
6,000	3	2	0	0	0	0	2	2[a]	0	0	0	1[a]	0	0	0	1[a]	0
Total	13	11	2	0	0	0	5	4	0	1	0	2	1	1	0	4	0

[a] DLT

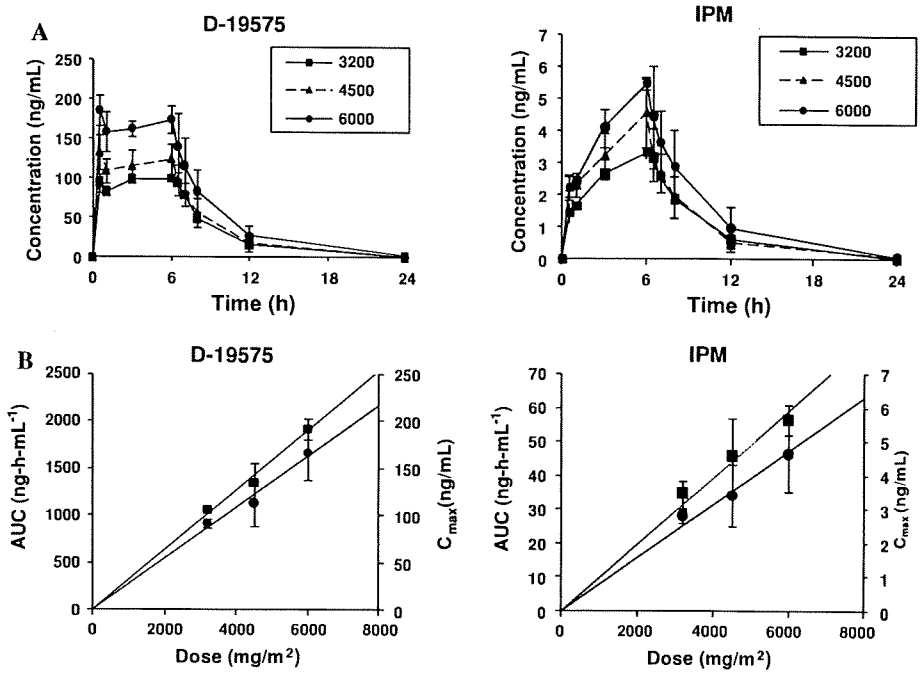

Fig. 2 Time course of the mean plasma concentrations of D-19575 and IPM after a single intravenous infusion of D-19575 (3,200, 4,500, or 6,000 mg/m^2) over 6 h (**a**) and the relations between the $AUC_{0-\infty}$ or C_{max} of D-19575 or IPM and the dose of D-19575 (**b**) for the first cycle of treatment. Data are means ± SD

of single doses of 3,200, 4,500, or 6,000 mg/m^2, but both D-19575 and IPM exhibited linear pharmacokinetics over the dose range studied (Fig. 2b). Pharmacokinetic parameters for D-19575 and IPM are summarized by dose of D-19575 in Tables 5 and 6, respectively. The mean C_{max} values of D-19575 were 107–192 ng/mL and were achieved at 2.46–3.33 h, with the mean $t_{1/2}$ values ranging from 2.30 to 2.53 h. D-19575 exhibited low CL_{tot} values [3.47–4.08 L/(h m^2)] as well as V_{ss} values (8.94–9.76 L/m^2) that were approximately equal to the volume of extracellular fluid. The plasma levels of IPM were smaller than those of D-19575 by a factor of ~25–30. The mean C_{max} values of IPM were 3.46–5.65 ng/mL and were achieved in 6.04–6.59 h, with mean $t_{1/2}$ values being similar to those for D-19575 and ranging between 2.38 and 2.66 h. There was no difference in pharmacokinetic data between cycles 1 and 2 for either D-19575 or IPM (data not shown).

Table 5 Mean pharmacokinetic parameters of D-19575 in plasma after a 6 h intravenous infusion of the indicated doses of D-19575 during cycle 1

Dose (mg/m^2)	No. of patients	$AUC_{0-\infty}$ (ng h/mL)		C_{max} (ng/mL)		$t_{1/2}$ (h)		CL_{tot} [L/(h m^2)]		V_{ss} (L/m^2)	
		Mean	SD	Mean	SD	Mean	SD	Mean	SD	Mean	SD
3,200	3	914	43.6	107	2.65	2.38	0.07	3.47	0.18	8.94	0.74
4,500	7	1,130	239	135	21.0	2.30	0.34	4.08	0.86	9.76	1.37
6,000	3	1,659	276	192	11.0	2.53	0.34	3.65	0.70	9.71	1.43

Table 6 Mean pharmacokinetic parameters of IPM in plasma after a 6 h intravenous infusion of the indicated doses of D-19575 during cycle 1

Dose (mg/m^2)	No. of patients	$AUC_{0-\infty}$ (ng h/mL)		C_{max} (ng/mL)		$t_{1/2}$ (h)	
		Mean	SD	Mean	SD	Mean	SD
3,200	3	28.1	2.04	3.46	0.39	2.38	0.06
4,500	7	34.0	8.84	4.58	1.11	2.47	0.37
6,000	3	46.5	11.2	5.65	0.43	2.66	0.45

Antitumor activity

Among all 13 patients evaluable for response, evidence of antitumor activity was observed in nine individuals, with one partial response and eight subjects showing stabilization of disease (Table 7). A 65-year-old female patient with advanced gallbladder cancer who had been treated with fluorouracil, cisplatin, and gemcitabine achieved a partial response that persisted for >5 months after two cycles of treatment with D-19575 at 4,500 mg/m^2 (Fig. 3). Stable disease was confirmed in four patients with colorectal cancer, one with gastric cancer, one with thymic cancer, one with thymoma, and one with non-small cell lung cancer.

Discussion

D-19575 has been developed as a new-generation cytotoxic alkylating agent whose activity is due in part to the preferential use of glucose by malignant cells [9]. We have now performed a dose-escalation phase I study of D-19575 in patients with solid tumors for evaluation of the safety and pharmacokinetics of this drug. Previous clinical trials with D-19575 were conducted given as short 1 h infusion schedule [10, 11]. However, taking into account the cellular uptake and cleavage of D-19575, a more continuous infusion schedule seemed to be preferable. Indeed, a previous pharmacokinetic analysis found that biphasic (fast–slow) intravenous infusion schedule produced the desired profile of a rapidly achieved and sustained plasma concentration for more than 6 h [12]. Based on the data, we have also employed a two-step, fast/slow 6 h infusion of D-19575 to rapidly achieve steady-state concentrations and expose tumor cells to the study drug over a moderately prolonged time. The MTD was determined to be 6,000 mg/m^2, with the recommended dose for phase II studies being 4,500 mg/m^2. DLTs included hypophosphatemia, hypokalemia, and metabolic acidosis, all of which are presentations of nephrotoxicity. In animals treated with D-19575, nephrotoxicity was evidenced histologically by a focal vacuolization of proximal tubules and a diffuse dilation of distal tubules (data on file; ASTA Medica AG, Germany). A major advantage of D-19575 over IFO is that treatment with D-19575 does not require administration of sodium mercaptoethanesulfonate for protection against urothelial toxicity. Two recent phase II trials performed by the European Organization for Research and Treatment of Cancer (EORTC)—New Drug Development Group [10, 11], demonstrated that active hydration did not show any nephroprotective effect toward D-19575 by reducing the contact time of tubule cells with the drug. On the basis of these results, active hydration was not used routinely in our study. Despite concerns for potential renal dysfunction with D-19575, creatinine clearance did not undergo a substantial decline in any of the treated patients (data not shown).

The initial activation reaction in IFO metabolism that gives rise to antitumor activity is mediated predominantly by the cytochrome P450 enzyme CYP3A4. The oxidation

Table 7 Antitumor activity of D-19575

Response	No of patients (%)
Partial response	1 (8)[a]
Stable disease	8 (62)[b]
Progressive disease	4 (30)
Not evaluable[c]	0 (0)

[a] Dose of 4,500 mg/m^2

[b] Two patients at a dose of 3,200 mg/m^2, four patients at 4,500 mg/m^2, and two patients at 6,000 mg/m^2

[c] Not assessed for response

Fig. 3 Representative computed tomography images illustrating response in patient with gallbladder cancer: Tumor shrinkage in cervical lymph node metastasis (**a**, **b**) and multiple liver metastases (**c**, **d**)

of IFO occurs via two major routes: (1) at the cyclic C-4, resulting in the formation of 4-OH-IFO, which is then decomposed to the cytotoxic metabolite IPM [13] and acrolein; and (2) through side-chain dechlorethylation, resulting in the formation of chloroacetaldehyde [14]. We have now shown that the plasma levels of IPM were smaller than those of D-19575 by a factor of ~25–30 in patients treated with D-19575. The $AUC_{0-\infty}$ for IPM increased in a dose-proportional manner within the range of 28.1–46.5 ng h/mL, values that are markedly higher than those achieved for IPM generated from IFO after bolus administration (mean of 11.9 ng h/mL) or continuous infusion (mean of 17.8 ng h/mL) in conventional treatment of soft tissue sarcoma [15]. These pharmacokinetic data suggest that infusion of D-19575 allows the safe achievement of higher concentrations of IPM compared with those achieved with standard IFO therapy. We also obtained no evidence of a relation between pharmacokinetic parameters and the occurrence of renal toxicity in the present study.

The intracellular uptake of D-19575 is mediated by the facilitative glucose transporters GLUT1 to GLUT5, the sodium-dependent glucose transporters SGLT1 and SGLT2, and, possibly, other transporter proteins. Increased rates of glucose transport and glycolysis are characteristic features of malignant transformed cells that result in part from overexpression of glucose transporters [16–19]. Overexpression of GLUT1 to GLUT3 has been detected in a wide range of human cancers, most prominently in those of breast, colon, and liver, with the extent of overexpression generally being inversely correlated with prognosis [20–22]. Its uptake mechanism, coupled with the increased metabolic rate of tumor cells, may contribute the chemotherapeutic activity of D-19575. The level of GLUT1 expression in tumors has been shown to be positively correlated with 2-[^{18}F]fluoro-2-deoxy-D-glucose uptake, semiquantified as standardized uptake value in positron emission tomography [23–26], suggesting that the latter parameter may be a suitable noninvasive biomarker for the sensitivity of cancers to D-19575.

In conclusion, the results of our phase I study suggest that D-19575 can be safely administered at a dose of 4,500 mg/m^2 by infusion over 6 h every 3 weeks to Japanese patients with advanced solid malignancies. They further suggest that this drug may prove clinically effective when administered as a single agent. The AUCs for IPM generated by D-19575 were found to be markedly higher than those achieved by administration of IFO, suggesting that infusion of D-19575 allows the safe achievement of higher concentrations of IPM compared with those generated by administration of IFO according to widespread clinical practice. The safety profile and the potential broad-spectrum efficacy of D-19575 thus warrant additional clinical evaluation of this new alkylating agent.

References

1. Seker H, Bertram B, Burkle A, Kaina B, Pohl J, Koepsell H, Wiesser M (2000) Mechanistic aspects of the cytotoxic activity of glufosfamide, a new tumour therapeutic agent. Br J Cancer 82(3):629–634
2. Liang J, Huang M, Duan W, Yu XQ, Zhou S (2007) Design of new oxazaphosphorine anticancer drugs. Curr Pharm Des 13(9):963–978

3. Younes M, Lechago LV, Somoano JR, Mosharaf M, Lechago J (1996) Wide expression of the human erythrocyte glucose transporter Glut1 in human cancers. Cancer Res 56(5):1164–1167
4. Yamamoto T, Seino Y, Fukumoto H, Koh G, Yano H, Inagaki N, Yamada Y, Inoue K, Manabe T, Imura H (1990) Over-expression of facilitative glucose transporter genes in human cancer. Biochem Biophys Res Commun 170(1):223–230
5. Veyhl M, Wagner K, Volk C, Gorboulev V, Baumgarten K, Weber WM, Schaper M, Bertram B, Wiessler M, Koepsell H (1998) Transport of the new chemotherapeutic agent beta-D-glucosylisophosphoramide mustard (D-19575) into tumor cells is mediated by the Na+-D-glucose cotransporter SAAT1. Proc Natl Acad Sci USA 95(6):2914–2919
6. Kong CT, Yet SF, Lever JE (1993) Cloning and expression of a mammalian Na+/amino acid cotransporter with sequence similarity to Na+/glucose cotransporters. J Biol Chem 268(3):1509–1512
7. Mackenzie B, Panayotova-Heiermann M, Loo DD, Lever JE, Wright EM (1994) SAAT1 is a low affinity Na+/glucose cotransporter and not an amino acid transporter. A reinterpretation. J Biol Chem 269(36):22488–22491
8. Stuben J, Port R, Bertram B, Bollow U, Hull WE, Schaper M, Pohl J, Wiessler M (1996) Pharmacokinetics and whole-body distribution of the new chemotherapeutic agent beta-D-glucosylisophosphoramide mustard and its effects on the incorporation of [methyl-3H]-thymidine in various tissues of the rat. Cancer Chemother Pharmacol 38(4):355–365
9. Storme T, Deroussent A, Mercier L, Prost E, Re M, Munier F, Martens T, Bourget P, Vassal G, Royer J (2009) New ifosfamide analogues designed for lower associated neurotoxicity and nephrotoxicity with modified alkylating kinetics leading to enhanced in vitro anticancer activity. J Pharmacol Exp Ther 328(2):598–609
10. Briasoulis E, Pavlidis N, Terret C, Bauer J, Fiedler W, Schoffski P, Raoul JL, Hess D, Selvais R, Lacombe D (2003) Glufosfamide administered using a 1-hour infusion given as first-line treatment for advanced pancreatic cancer. A phase II trial of the EORTC-new drug development group. Eur J Cancer 39(16):2334–2340
11. Giaccone G, Smit EF, de Jonge M, Dansin E, Briasoulis E, Ardizzoni A, Douillard JY, Spaeth D, Lacombe D, Baron B (2004) Glufosfamide administered by 1-hour infusion as a second-line treatment for advanced non-small cell lung cancer; a phase II trial of the EORTC-New Drug Development Group. Eur J Cancer 40(5):667–672
12. Briasoulis E, Judson I, Pavlidis N, Beale P, Wanders J, Groot Y, Veerman G, Schuessler M, Niebch G, Siamopoulos K (2000) Phase I trial of 6-h infusion of glufosfamide, a new alkylating agent with potentially enhanced selectivity for tumors that overexpress transmembrane glucose transporters: a study of the European Organization for Research and Treatment of Cancer Early Clinical Studies Group. J Clin Oncol 18(20):3535–3544
13. Germann N, Urien S, Rodgers AH, Ratterree M, Struck RF, Waud WR, Serota DG, Bastian G, Jursic BS, Morgan LR (2005) Comparative preclinical toxicology and pharmacology of isophosphoramide mustard, the active metabolite of ifosfamide. Cancer Chemother Pharmacol 55(2):143–151
14. Boddy AV, Yule SM (2000) Metabolism and pharmacokinetics of oxazaphosphorines. Clin Pharmacokinet 38(4):291–304
15. Boddy AV, Yule SM, Wyllie R, Price L, Pearson AD, Idle JR (1995) Comparison of continuous infusion and bolus administration of ifosfamide in children. Eur J Cancer 31A(5):785–790
16. Rempel A, Mathupala SP, Griffin CA, Hawkins AL, Pedersen PL (1996) Glucose catabolism in cancer cells: amplification of the gene encoding type II hexokinase. Cancer Res 56(11):2468–2471
17. Lundholm K, Edstrom S, Karlberg I, Ekman L, Schersten T (1982) Glucose turnover, gluconeogenesis from glycerol, and estimation of net glucose cycling in cancer patients. Cancer 50(6):1142–1150
18. Elsas LJ, Longo N (1992) Glucose transporters. Annu Rev Med 43:377–393
19. Hediger MA, Rhoads DB (1994) Molecular physiology of sodium–glucose cotransporters. Physiol Rev 74(4):993–1026
20. Brown RS, Wahl RL (1993) Overexpression of Glut-1 glucose transporter in human breast cancer. An immunohistochemical study. Cancer 72(10):2979–2985
21. Grover-McKay M, Walsh SA, Seftor EA, Thomas PA, Hendrix MJ (1998) Role for glucose transporter 1 protein in human breast cancer. Pathol Oncol Res 4(2):115–120
22. Haber RS, Rathan A, Weiser KR, Pritsker A, Itzkowitz SH, Bodian C, Slater G, Weiss A, Burstein DE (1998) GLUT1 glucose transporter expression in colorectal carcinoma: a marker for poor prognosis. Cancer 83(1):34–40
23. Gu J, Yamamoto H, Fukunaga H, Danno K, Takemasa I, Ikeda M, Tatsumi M, Sekimoto M, Hatazawa J, Nishimura T (2006) Correlation of GLUT-1 overexpression, tumor size, and depth of invasion with 18F–2-fluoro-2-deoxy-D-glucose uptake by positron emission tomography in colorectal cancer. Dig Dis Sci 51(12):2198–2205
24. Yamada A, Oguchi K, Fukushima M, Imai Y, Kadoya M (2006) Evaluation of 2-deoxy-2-[18F]fluoro-D-glucose positron emission tomography in gastric carcinoma: relation to histological subtypes, depth of tumor invasion, and glucose transporter-1 expression. Ann Nucl Med 20(9):597–604
25. Brown RS, Leung JY, Fisher SJ, Frey KA, Ethier SP, Wahl RL (1996) Intratumoral distribution of tritiated-FDG in breast carcinoma: correlation between Glut-1 expression and FDG uptake. J Nucl Med 37(6):1042–1047
26. Brown RS, Leung JY, Kison PV, Zasadny KR, Flint A, Wahl RL (1999) Glucose transporters and FDG uptake in untreated primary human non-small cell lung cancer. J Nucl Med 40(4):556–565

De Novo Resistance to Epidermal Growth Factor Receptor-Tyrosine Kinase Inhibitors in *EGFR* Mutation-Positive Patients with Non-small Cell Lung Cancer

Masayuki Takeda, MD, PhD, Isamu Okamoto, MD, PhD,* Yoshihiko Fujita, PhD,† Tokuzo Arao, MD, PhD,† Hiroyuki Ito, MD, PhD,‡ Masahiro Fukuoka, MD, PhD,§ Kazuto Nishio, MD, PhD,† and Kazuhiko Nakagawa, MD, PhD**

Background: Somatic mutations in the epidermal growth factor receptor (EGFR) gene are a predictor of response to treatment with EGFR tyrosine kinase inhibitors (TKIs) in patients with non-small cell lung cancer (NSCLC). However, mechanisms of de novo resistance to these drugs in patients harboring *EGFR* mutations have remained unclear. We examined whether the mutational status of *KRAS* might be associated with primary resistance to EGFR-TKIs in *EGFR* mutation-positive patients with NSCLC.

Methods: Forty patients with NSCLC with *EGFR* mutations who were treated with gefitinib or erlotinib and had archival tissue specimens available were enrolled in the study. *KRAS* mutations were analyzed by direct sequencing.

Results: Three (7.5%) of the 40 patients had progressive disease, and two (67%) of these three individuals had both *KRAS* and *EGFR* mutations.

Conclusions: Our results suggest that *KRAS* mutation is a negative predictor of response to EGFR-TKIs in *EGFR* mutation-positive patients with NSCLC.

Key Words: Drug resistance, Epidermal growth factor receptor, KRAS, Non-small cell lung cancer, EGFR-TKI.

(*J Thorac Oncol.* 2010;5: 399–400)

A total of 40 patients with non-small cell lung cancer (NSCLC) harboring epidermal growth factor receptor (*EGFR*) mutations were treated with gefitinib (n = 36) or erlotinib (n = 4) between September 2002 and January 2009, and three patients exhibited resistance to EGFR-tyrosine kinase inhibitor (TKIs). (i) Case 1 was a 63-year-old man who had never smoked and was diagnosed with lung adenocarcinoma of stage IV. Molecular screening identified a deletion mutation in exon 19 of *EGFR*, and he had received gefitinib as the second-line therapy. Although he tolerated gefitinib well, the primary lung lesion showed slow but steady growth, and he was removed from therapy because of his progressive disease (PD) at day 58 (Figure 1*A*). (ii) Case 2 was a 69-year-old man who had never smoked, had adenocarcinoma of stage IIIB, harbored a deletion in exon 19 of *EGFR*, and was treated with erlotinib as the third-line therapy. A chest computed tomography scan on day 28 revealed enlargement of the primary lung lesion, and the case was subsequently classified as PD (Figure 1*B*). (iii) Case 3 was a 52-year-old man who was a current smoker, had lung adenocarcinoma of stage IV with left adrenal metastasis, harbored a deletion in exon 19 of *EGFR*, and received erlotinib as the fourth-line therapy. Chest computed tomography on day 32 showed enlargement of the left adrenal metastasis, resulting in a classification of PD (Figure 1*C*). Thus, these clinical data demonstrated the existence of de novo resistance to EGFR-TKIs in *EGFR* mutation-positive patients. We examined the mutational status of *KRAS* in the three patients who showed PD as their best response. An amino acid substitution at codon 12 (G12D) of *KRAS* was identified in two of these three patients (Figure 1*D–F*).

DISCUSSION

Somatic mutations of the *EGFR* gene are associated with an increased response to EGFR-TKI in patients with NSCLC. Several prospective clinical trials of EGFR-TKI treatment for patients with NSCLC with *EGFR* mutations have subsequently revealed radiographic response rates of 55 to 91%. It remains of clinical concern, however, that a small proportion of patients with NSCLC with *EGFR* mutations show de novo resistance to EGFR-TKIs and that molecular markers to predict a lack of response to these drugs remain to be identified. We have now examined *KRAS* mutation status in *EGFR* mutation-positive patients with NSCLC treated with EGFR-TKIs and found a high incidence of concomitant *KRAS* mutation in individuals who did not respond to these drugs. Our results indicate that *KRAS* mutation may be clinically useful as a negative predictive marker of sensitivity to EGFR-TKIs in patients with NSCLC with *EGFR* mutations. Previous studies have also shown that *KRAS* mutations are associated with resistance to EGFR-TKIs in patients with NSCLC and that *EGFR* and *KRAS* mutations

Departments of *Medical Oncology, †Genome Biology, and ‡Pathology, Kinki University School of Medicine, Osaka-Sayama; and §Department of Medical Oncology, Kinki University School of Medicine, Sakai Hospital, Minami-ku, Sakai, Osaka, Japan.

Disclosure: The authors declare no conflict of interest.

Address for correspondence: Isamu Okamoto, Department of Medical Oncology, Kinki University School of Medicine, 377-2 Ohno-higashi, Osaka-Sayama, Osaka 589-8511, Japan. E-mail: chi-okamoto@dotd.med.kindai.ac.jp

ISSN: 1556-0864/10/0503-0399

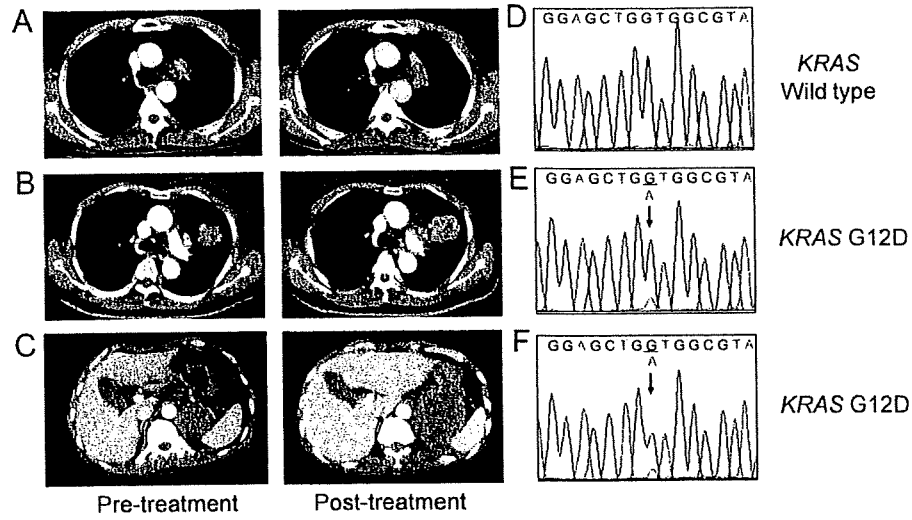

FIGURE 1. Clinical and molecular characteristics of patients with non-small cell lung cancer (NSCLC) who showed de novo resistance to epidermal growth factor receptor-tyrosine kinase inhibitors (EGFR-TKIs). *A–C*, Computed tomography (CT) images obtained before and after EGFR-TKI treatment for cases 1 to 3, respectively. *D–F*, Sequence chromatographs of *KRAS* mutation status determined with tumor tissue isolated before EGFR-TKI treatment for cases 1 to 3, respectively. Arrows indicate the mutated nucleotide (G→A) in codon 12 for cases 2 and 3.

appear to be mutually exclusive in such patients,[1–3] suggesting that *KRAS* mutations are predictors of unresponsiveness to EGFR-TKIs in patients with NSCLC with wild-type *EGFR*. The mutual exclusivity of *EGFR* and *KRAS* mutations combined with their prevalence patterns in lung adenocarcinoma, with *KRAS* mutations being preferentially found in smokers and *EGFR* mutations in nonsmokers, suggests that the mutations in these two genes might arise through different pathogenic pathways. Conversely, some studies have shown that *KRAS* mutations do sometimes coexist with *EGFR* mutations in patients with NSCLC.[4,5] The extent of coexistence of *EGFR* and *KRAS* mutations in NSCLC thus remains unclear, in large part as a result of the low frequency of *KRAS* mutations, and the clinical relevance of *KRAS* mutations in *EGFR* mutation-positive patients has remained unknown. We have now shown that patients with NSCLC harboring *EGFR* mutations who exhibit de novo resistance to EGFR-TKIs have a high incidence of *KRAS* mutation, suggesting that the presence of *KRAS* mutations might provide a basis for the identification of *EGFR* mutation-positive patients who are unlikely to benefit from EGFR-TKI treatment. Our clinical findings are consistent with preclinical data showing that forced expression of mutant KRAS in PC-9 human NSCLC cells, which harbor an activating mutation of *EGFR*, resulted in a reduction in the sensitivity of these cells to gefitinib.[6] Gefitinib shuts down both PI3K-AKT and RAS-RAF-MEK-ERK signaling pathways in PC-9 cells; however, expression of the KRAS mutant resulted in constitutive activation of these signaling pathways in a manner independent of EGFR activation, leading to continued cell growth and survival.

In July 2009, gefitinib received a license from the European Medicines Agency for all lines of therapy in patients with locally advanced or metastatic NSCLC positive for activating mutations of *EGFR*. More patients with *EGFR* mutation-positive tumors will thus now receive EGFR-TKIs. Our present results suggest that EGFR-TKIs should not be given routinely to patients harboring concomitant *KRAS* and *EGFR* mutations. In the event that such patients do receive treatment with EGFR-TKIs, they should be followed up after a short interval to obtain early evidence of possible tumor progression.

KRAS mutations cannot account for all cases of de novo resistance to EGFR-TKIs in *EGFR* mutation-positive patients with NSCLC. A recent study showed that loss of *PTEN* contributes to erlotinib resistance in an *EGFR* mutation-positive NSCLC cell line.[7] Loss of *PTEN* resulted in partial uncoupling of the mutant EGFR from downstream signaling and further activated the receptor, leading to erlotinib resistance. Both homozygous deletion of *PTEN* and *EGFR* mutation were detected in one of 24 clinical specimens of NSCLC with *EGFR* mutations, although the efficacy of EGFR-TKIs was not evaluated in the corresponding patient.

In conclusion, our results suggest that *KRAS* mutation status should be assessed before initiation of EGFR-TKI treatment in *EGFR* mutation-positive patients with NSCLC, allowing enrichment of the population of such patients who are likely to prove responsive to the treatment.

ACKNOWLEDGMENTS

The authors thank Tadao Uesugi for technical assistance.

REFERENCES

1. Shigematsu H, Lin L, Takahashi T, et al. Clinical and biological features associated with epidermal growth factor receptor gene mutations in lung cancers. *J Natl Cancer Inst* 2005;97:339–346.
2. Pao W, Wang TY, Riely GJ, et al. KRAS mutations and primary resistance of lung adenocarcinomas to gefitinib or erlotinib. *PLoS Med* 2005;2:e17.
3. Kosaka T, Yatabe Y, Endoh H, et al. Mutations of the epidermal growth factor receptor gene in lung cancer: biological and clinical implications. *Cancer Res* 2004;64:8919–8923.
4. Kalikaki A, Koutsopoulos A, Trypaki M, et al. Comparison of EGFR and K-RAS gene status between primary tumours and corresponding metastases in NSCLC. *Br J Cancer* 2008;99:923–929.
5. Han SW, Kim TY, Jeon YK, et al. Optimization of patient selection for gefitinib in non-small cell lung cancer by combined analysis of epidermal growth factor receptor mutation, K-ras mutation, and Akt phosphorylation. *Clin Cancer Res* 2006;12:2538–2544.
6. Uchida A, Hirano S, Kitao H, et al. Activation of downstream epidermal growth factor receptor (EGFR) signaling provides gefitinib-resistance in cells carrying EGFR mutation. *Cancer Sci* 2007;98:357–363.
7. Sos ML, Koker M, Weir BA, et al. PTEN loss contributes to erlotinib resistance in EGFR-mutant lung cancer by activation of Akt and EGFR. *Cancer Res* 2009;69:3256–3261.

Sorafenib Inhibits Non–Small Cell Lung Cancer Cell Growth by Targeting B-RAF in *KRAS* Wild-Type Cells and C-RAF in *KRAS* Mutant Cells

Ken Takezawa,[1] Isamu Okamoto,[1] Kimio Yonesaka,[1] Erina Hatashita,[1] Yuki Yamada,[1] Masahiro Fukuoka,[2] and Kazuhiko Nakagawa[1]

[1]Department of Medical Oncology, Kinki University School of Medicine; [2]Department of Medical Oncology, Kinki University School of Medicine, Sakai Hospital, Osaka, Japan

Abstract

Sorafenib is a multikinase inhibitor whose targets include B-RAF and C-RAF, both of which function in the extracellular signal-regulated kinase (ERK) signaling pathway but which also have distinct downstream targets. The relative effects of sorafenib on B-RAF and C-RAF signaling in tumor cells remain unclear, however. We have now examined the effects of sorafenib as well as of B-RAF or C-RAF depletion by RNA interference on cell growth and ERK signaling in non–small cell lung cancer (NSCLC) cell lines with or without *KRAS* mutations. Sorafenib inhibited ERK phosphorylation in cells with wild-type *KRAS* but not in those with mutant *KRAS*. Despite this difference, sorafenib inhibited cell growth and induced G_1 arrest in both cell types. Depletion of B-RAF, but not that of C-RAF, inhibited ERK phosphorylation as well as suppressed cell growth and induced G_1 arrest in cells with wild-type *KRAS*. In contrast, depletion of C-RAF inhibited cell growth and induced G_1 arrest, without affecting ERK phosphorylation, in cells with mutant *KRAS*; depletion of B-RAF did not induce G_1 arrest in these cells. These data suggest that B-RAF-ERK signaling and C-RAF signaling play the dominant roles in regulation of cell growth in NSCLC cells with wild-type or mutant *KRAS*, respectively. The G_1 arrest induced by either C-RAF depletion or sorafenib in cells with mutant *KRAS* was associated with down-regulation of cyclin E. Our results thus suggest that sorafenib inhibits NSCLC cell growth by targeting B-RAF in cells with wild-type *KRAS* and C-RAF in those with mutant *KRAS*. [Cancer Res 2009;69(16):6515–21]

Introduction

Lung cancer is the leading cause of cancer-related mortality worldwide (1). Treatment options are limited for patients with advanced metastatic lung cancer, with traditional cytotoxic chemotherapy conferring only a limited survival benefit. Target-based therapies are therefore being pursued as potential treatment alternatives. The RAS-RAF-mitogen-activated protein kinase (MAPK)/extracellular signal-regulated kinase (ERK) kinase-ERK signaling pathway is a promising therapeutic target given its central role in regulation of mammalian cell proliferation, relaying extracellular signals from ligand-bound receptor tyrosine kinases (RTK) at the cell surface to the nucleus via a cascade of specific phosphorylation events and beginning with the activation of the small GTPase RAS (2). Much attention is thus being focused on the development of inhibitors of this pathway.

RAF was the first effector kinase downstream of RAS to be identified (3). To date, the most successful clinical inhibitor of RAF activity is sorafenib (Nexavar, BAY 43-9006), an orally available compound that has received approval by the U.S. Food and Drug Administration for the treatment of advanced renal cell carcinoma and hepatocellular carcinoma. Sorafenib is also currently undergoing clinical evaluation for a variety of additional cancers, including non–small cell lung cancer (NSCLC; refs. 4–7).

The mutational status of *RAS* and *B-RAF* genes is thought to affect the sensitivity of tumor cell lines to sorafenib as a result of the inappropriate activation by such mutations of the MAPK pathway mediated by ERK (8, 9). The sensitivity of tumor cell lines with different *RAS* mutations to sorafenib is less well characterized than is that of those with *B-RAF* mutations (10–14). Despite promising results of clinical trials of sorafenib monotherapy in NSCLC patients (4–7), little is known of the possible differences in the sorafenib sensitivity of NSCLC cells according to the mutational status of *KRAS*. We have therefore now examined the effects of RAF inhibition on the growth of NSCLC cells with or without *KRAS* mutations and further investigated the mechanisms of such effects.

Materials and Methods

Cell culture and reagents. The human NSCLC cell lines NCI-H292 (H292), LK-2, Sq-1, NCI-H520 (H520), PC9, NCI-H1650 (H1650), HCC827, NCI-H1975 (H1975), A549, NCI-H460 (H460), NCI-H23 (H23), NCI-H358 (H358), and NCI-H1299 (H1299) were obtained from the American Type Culture Collection. Ma70 cells were obtained as previously described (15). All cells were cultured under a humidified atmosphere of 5% CO_2 at 37°C in RPMI 1640 (Sigma) supplemented with 10% fetal bovine serum. Sorafenib was kindly provided by Bayer Pharmaceutical, dissolved in DMSO, and stored in aliquots at −20°C.

Assay of anchorage-dependent cell growth [3-(4,5-dimethylthiazol-2-yl)-2,5-diphenyltetrazolium bromide assay]. Cells were plated in 96-well flat-bottomed plates and cultured for 24 h before exposure to various concentrations of sorafenib for 72 h. TetraColor One (5 mmol/L tetrazolium monosodium salt and 0.2 mmol/L 1-methoxy-5-methyl phenazinium methylsulfate; Seikagaku) was then added to each well, and the cells were incubated for 3 h at 37°C before measurement of absorbance at 490 nm with a Multiskan Spectrum instrument (Thermo Labsystems). Absorbance values were expressed as a percentage of that for untreated cells, and the concentration of sorafenib resulting in 50% growth inhibition (IC_{50}) was calculated.

Assay of anchorage-independent colony formation in soft agar. Anchorage-independent cell proliferation in soft agar was assayed with the use of a CytoSelect 96-Well Cell Transformation Assay (Cell Biolabs). In brief, cells were cultured for 7 d in complete medium containing soft agar and various concentrations of sorafenib. The agar matrix was then solubilized, the cells were stained with 3-(4,5-dimethylthiazol-2-yl)-2,5-diphenyltetrazolium

Requests for reprints: Isamu Okamoto, Department of Medical Oncology, Kinki University School of Medicine, 377-2 Ohno-higashi, Osaka-Sayama, Osaka 589-8511, Japan. Phone: 81-72-366-0221; Fax: 81-72-360-5000; E-mail: chi-okamoto@dotd.med.kindai.ac.jp.

doi:10.1158/0008-5472.CAN-09-1076

bromide (MTT) and lysed, and the absorbance at 570 nm was measured relative to that at a reference wavelength of 690 nm. Normalized absorbance values were expressed as a percentage of that for untreated cells, and the IC_{50} of sorafenib for inhibition of colony formation was calculated.

Cell cycle analysis. Cells were harvested, washed with PBS, fixed with 70% methanol, washed again with PBS, and stained with propidium iodide (0.05 mg/mL) in a solution containing 0.1% Triton X-100, 0.1 mmol/L EDTA, and RNase A (0.05 mg/mL). The stained cells ($\sim 1 \times 10^6$) were then analyzed for DNA content with a flow cytometer (FACSCalibur, Becton Dickinson) and ModFit software (Verity Software House).

Immunoblot analysis. Cells were washed twice with ice-cold PBS and then lysed in a solution containing 20 mmol/L Tris-HCl (pH 7.5), 150 mmol/L NaCl, 1 mmol/L EDTA, 1% Triton X-100, 2.5 mmol/L sodium pyrophosphate, 1 mmol/L phenylmethylsulfonyl fluoride, and 1 μg/mL leupeptin. The protein concentration of lysates was determined with the Bradford reagent (Bio-Rad), and equal amounts of protein were subjected to SDS-PAGE on a 7.5% gel. The separated proteins were transferred to a nitrocellulose membrane, which was then exposed to 5% nonfat dried milk in PBS for 1 h at room temperature before incubation overnight at 4°C with rabbit polyclonal antibodies to human phosphorylated ERK (1:1,000 dilution; Santa Cruz Biotechnology), ERK (1:1,000 dilution; Santa Cruz Biotechnology), FLAG epitope (1:1,000 dilution; Cell Signaling Technology), B-RAF (1:1,000 dilution; Santa Cruz Biotechnology), C-RAF (1:1,000 dilution; Cell Signaling Technology), or β-actin (1:500 dilution; Sigma) or with mouse monoclonal antibodies to cyclin E (1:1,000 dilution; Santa Cruz Biotechnology). The membrane was then washed with PBS containing 0.05% Tween 20 before incubation for 1 h at room temperature with horseradish peroxidase–conjugated goat antibodies to rabbit (Sigma) or mouse (Santa Cruz Biotechnology) immunoglobulin G. Immune complexes were finally detected with chemiluminescence reagents (Perkin-Elmer Life Science).

Forced expression of KRAS-V12. An expression vector for FLAG-tagged human KRAS-V12 was constructed by inserting the corresponding cDNA into the pcDNA3 plasmid (Invitrogen). The expression vector was introduced into H1299 cells by transfection for 48 h with the use of the Lipofectamine 2000 reagent (Invitrogen).

Gene silencing. Cells were plated at 50% to 60% confluence in six-well plates or 25-cm^2 flasks and then incubated for 24 h before transient transfection for 48 h with small interfering RNAs (siRNAs) mixed with the Lipofectamine reagent. The siRNAs specific for B-RAF (5′-AGACAGGAAUCGAAUGAAA-3′) or C-RAF (5′-CCUCACGCCUUCACCUUUA-3′) mRNAs were obtained from Dharmacon, and a nonspecific siRNA (control) was obtained from Nippon EGT. The cells were then subjected to immunoblot analysis or flow cytometry.

Statistical analysis. Data were analyzed by Student's two-tailed *t* test. A *P* value of <0.05 was considered statistically significant.

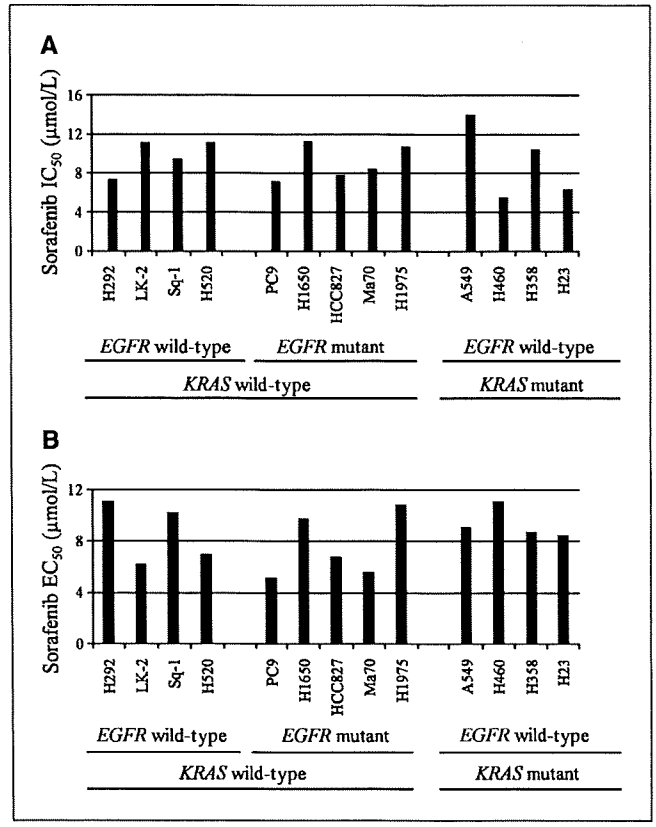

Figure 1. Effects of sorafenib on the growth of NSCLC cell lines classified according to *KRAS* and *EGFR* mutational status. *A*, the indicated NSCLC cell lines were cultured for 72 h in complete culture medium containing various concentrations of sorafenib, after which cell viability was assessed with the MTT assay and the IC_{50} values of sorafenib for inhibition of cell growth were determined. *B*, the indicated NSCLC cell lines were cultured for 7 d in complete medium containing soft agar and various concentrations of sorafenib, after which colony formation was evaluated and the IC_{50} values of sorafenib for inhibition of anchorage-independent cell proliferation were determined. All data are means of triplicates from representative experiments that were repeated on three separate occasions.

Results

Sorafenib inhibits cell growth by inducing G_1 arrest in NSCLC cell lines independently of *KRAS* genotype. The various isoforms of RAF are the principal effectors of RAS in the ERK signaling pathway, and mutant RAS proteins trigger persistent activation of downstream effectors (3). To determine whether the mutational status of *KRAS* might affect the sensitivity of NSCLC cells to sorafenib, an inhibitor of the kinase activity of RAF (16), we first examined the effects of this drug on the anchorage-dependent growth of NSCLC cells with or without *KRAS* mutations by the MTT assay. Sorafenib inhibited cell growth with IC_{50} values ranging from 7.4 to 11.3 μmol/L in NSCLC cells with wild-type *KRAS* and from 5.6 to 14.1 μmol/L in those with mutant *KRAS* (Fig. 1*A*), values that are within the clinically relevant concentration range for this drug (17). This inhibitory effect of sorafenib in cells with wild-type *KRAS* also seemed to be independent of whether the cells contained a mutant version of the *epidermal growth factor receptor* (*EGFR*) gene. We next investigated the effects of sorafenib on anchorage-independent colony formation in soft agar, a more clinically relevant model of NSCLC cell proliferation. Sorafenib inhibited anchorage-independent colony formation with IC_{50} values of 5.6 to 11.1 μmol/L in cells with wild-type *KRAS* and of 8.5 to 11.1 μmol/L in those with mutant *KRAS* (Fig. 1*B*). These data thus indicated that sorafenib inhibits the growth of NSCLC cells in a manner independent of *KRAS* mutational status.

To investigate the mechanism by which sorafenib inhibits NSCLC cell growth, we examined the cell cycle profile by flow cytometry. Sorafenib increased the proportion of cells in G_1 phase of the cell cycle and reduced that of cells in S or G_2-M phases in all tested cell lines regardless of *KRAS* mutational status (Fig. 2). Sorafenib did not increase the proportion of cells in sub-G_1 phase, a characteristic of apoptosis. These data thus indicated that sorafenib inhibits cell growth by inducing arrest of the cell cycle in G_1 phase.

Effects of sorafenib on the ERK signaling pathway in NSCLC cell lines. To examine the effects of sorafenib on the ERK signaling pathway in NSCLC cells, we performed immunoblot analysis with antibodies specific for phosphorylated (activated) ERK. Sorafenib markedly inhibited ERK phosphorylation in cells with wild-type *KRAS* regardless of the mutational status of *EGFR* (Fig. 3*A*). In contrast, sorafenib had no effect on the level of ERK phosphorylation in cells

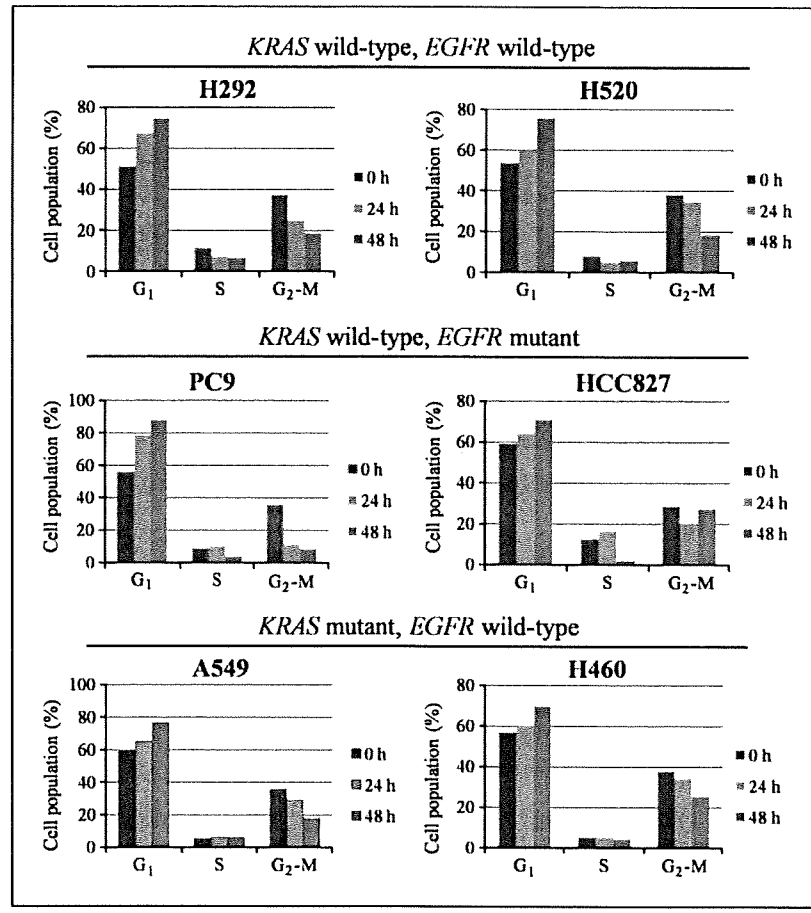

Figure 2. Effects of sorafenib on cell cycle distribution in NSCLC cells classified according to *KRAS* and *EGFR* status. Cells were incubated for 0, 24, or 48 h in complete culture medium containing 15 μmol/L sorafenib and were then fixed, stained with propidium iodide, and analyzed for cell cycle distribution by flow cytometry. All data are means of triplicates from representative experiments that were repeated on three separate occasions.

with mutant *KRAS*. To investigate further whether the effect of sorafenib on ERK phosphorylation is dependent on *KRAS* mutational status, we introduced an expression vector for FLAG epitope-tagged KRAS with the activating Val^{12} mutation (KRAS-V12) into the human NSCLC cell line H1299, which harbors wild-type endogenous *KRAS*. Whereas sorafenib inhibited ERK phosphorylation in nontransfected cells or cells transfected with the empty vector, it failed to do so in cells expressing KRAS-V12 (Fig. 3*B*). These results thus suggested that sorafenib blocks the ERK signaling pathway only in NSCLC cells harboring wild-type *KRAS*.

B-RAF but not C-RAF depletion inhibits ERK phosphorylation in NSCLC cells with wild-type or mutant KRAS. The mammalian RAF family includes A-RAF, B-RAF, and C-RAF, all of which function in the ERK pathway but also have different downstream phosphorylation targets and play distinct roles in signaling (18). Although suggested to be a B-RAF inhibitor, sorafenib inhibits the activity of C-RAF with a potency 4-fold that apparent for B-RAF (16). To investigate the downstream consequences of B-RAF and C-RAF signaling in NSCLC cells, we examined the effects of the depletion of these kinases with a siRNA-based approach. Immunoblot analysis revealed

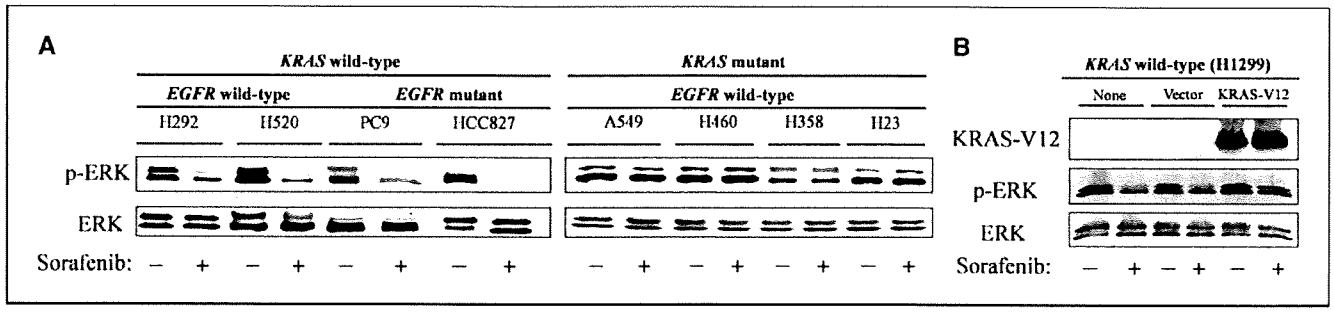

Figure 3. Effects of sorafenib on ERK phosphorylation in NSCLC cells classified according to *KRAS* and *EGFR* status. *A*, cells were incubated for 2 h in the presence or absence of sorafenib (15 μmol/L), after which cell lysates (25 μg of soluble protein) were subjected to immunoblot analysis with antibodies to phosphorylated (*p-ERK*) or total forms of ERK. *B*, H1299 cells were transiently transfected (or not) for 48 h with an expression vector for FLAG-tagged KRAS-V12 or with the corresponding empty vector and were then incubated for 2 h in the presence or absence of sorafenib (15 μmol/L). Cell lysates (25 μg of soluble protein) were then subjected to immunoblot analysis with antibodies to FLAG and to phosphorylated or total forms of ERK.

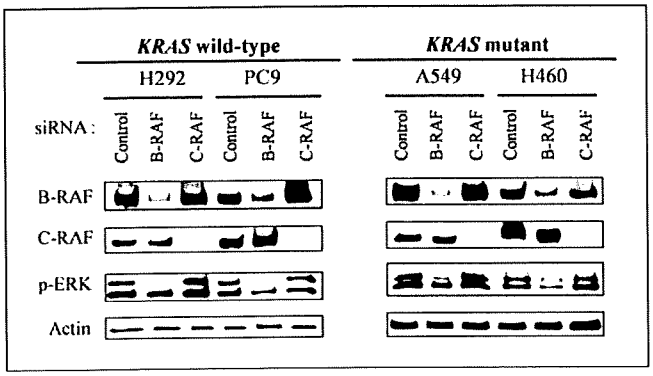

Figure 4. Effects of transient depletion of B-RAF or C-RAF on ERK phosphorylation in NSCLC cells. Cells harboring wild-type or mutant *KRAS* were transfected with nonspecific (control), B-RAF, or C-RAF siRNAs for 48 h, after which cell lysates were prepared and subjected to immunoblot analysis with antibodies to B-RAF, C-RAF, phosphorylated ERK, and β-actin (loading control).

that transfection of NSCLC cells with siRNAs specific for B-RAF or C-RAF mRNAs resulted in marked and selective depletion of the corresponding protein (Fig. 4). Such depletion of B-RAF resulted in inhibition of ERK phosphorylation in cells harboring wild-type or mutant *KRAS*, whereas depletion of C-RAF had no such effect (Fig. 4). These data thus suggested that depletion of B-RAF, but not that of C-RAF, inhibits ERK phosphorylation regardless of *KRAS* status.

Effects of RAF depletion on NSCLC cell proliferation. We next examined the effects of B-RAF or C-RAF depletion on NSCLC cell proliferation and cell cycle distribution. Depletion of B-RAF resulted in significant inhibition of cell proliferation (Fig. 5*A*) and an increase in the proportion of cells in G_1 phase of the cell cycle (Fig. 5*B*), whereas depletion of C-RAF had no such effects, in NSCLC cells harboring wild-type *KRAS*. In contrast, depletion of C-RAF induced significant inhibition of cell proliferation (Fig. 5*A*) and an increase in the proportion of cells in G_1 phase (Fig. 5*B*), whereas depletion of B-RAF had only a less pronounced effect on cell proliferation, in NSCLC cells with mutant *KRAS*. These data thus suggested that B-RAF-ERK signaling regulates cell proliferation in NSCLC cells with wild-type *KRAS*, whereas C-RAF signaling mediates such regulation in NSCLC cells with mutant *KRAS*.

Sorafenib or C-RAF depletion inhibits cyclin E expression in NSCLC cells with mutant *KRAS*. Finally, to characterize further the growth inhibition and G_1 arrest induced by C-RAF depletion or sorafenib in NSCLC cells with mutant *KRAS*, we examined the expression of cyclin E, an essential promoter of the transition from G_1 to S phase of the cell cycle (19). Immunoblot analysis revealed that depletion of C-RAF in A549 or H460 cells resulted in pronounced inhibition of cyclin E expression, whereas depletion of B-RAF had no such effect (Fig. 6). Exposure of the cells to sorafenib also induced loss of cyclin E (Fig. 6). These results thus suggest that the G_1 arrest induced by depletion of C-RAF or by sorafenib in NSCLC cells with mutant *KRAS* may be attributable to the down-regulation of cyclin E.

Discussion

RAS is an upstream component of the ERK signaling pathway, which is aberrantly activated by oncogenic mutations of RAS genes. Among RAS family genes, mutations of *KRAS* are most common in solid malignancies, including NSCLC (8, 20, 21). Indeed, *KRAS* mutations have been associated with poor prognosis and resistance to conventional cytotoxic chemotherapy in NSCLC (22–24). Whereas EGFR tyrosine kinase inhibitors are most efficacious in NSCLC patients with *EGFR* mutations, *KRAS* mutations are associated with resistance to these agents (25–28). The development of therapeutic strategies for NSCLC patients with *KRAS* mutations is thus an important clinical goal. RAF serine-threonine kinases are the principal effectors of RAS in the ERK signaling pathway. Given the key role of this pathway in tumor growth, RAF is a potential target for cancer therapy.

Sorafenib is an orally available compound that has been developed as a multikinase inhibitor with activity against RAF and several RTKs. The sensitivity of cancer cells to sorafenib might be expected to be affected by *KRAS* status, given that *KRAS* mutations result in activation of the ERK pathway (8). However, as far as we are aware, no previous study has compared sorafenib sensitivity among a panel of tumor cell lines of different *KRAS* mutational status. We have now evaluated the effects of sorafenib on the growth of NSCLC cells harboring wild-type or mutant forms of *KRAS* with two different assay systems, the MTT assay and anchorage-independent colony formation assay, given that previous studies have revealed differences in the sensitivity of cells to tested drugs between these two assay systems (29). The IC_{50} values for inhibition of cell growth by sorafenib in these assays have generally been found to be well below 15 μmol/L, the maximum achievable plasma concentration of this drug (17). We found that the potency of sorafenib for inhibition of cell growth was similar for NSCLC cells regardless of *KRAS* mutational status in both assay systems. We also performed a longer-term clonogenic survival assay and again found that sorafenib inhibited the survival of NSCLC cells regardless of *KRAS* status (data not shown). These results thus indicate that sorafenib inhibits the growth of NSCLC cells with mutant *KRAS* as well as it does that of those with wild-type *KRAS* in a clinically relevant concentration range.

We have shown that sorafenib inhibited ERK phosphorylation and induced G_1 arrest in NSCLC cells with wild-type *KRAS*, consistent with previous results obtained with several cancer cell lines harboring wild-type *KRAS* (13, 30, 31). Inhibition of the ERK signaling pathway, as reflected by a reduced level of ERK phosphorylation, results in inhibition of cell proliferation and induction of G_1 arrest in various cell types (32–35). In the present study, we found that depletion of B-RAF by RNA interference also inhibited ERK phosphorylation as well as attenuated cell proliferation and induced G_1 arrest in NSCLC cells with wild-type *KRAS*. These results suggest that inhibition of B-RAF-ERK signaling contributes to suppression of the growth of NSCLC cells harboring wild-type *KRAS* by sorafenib. Consistent with these findings, the specific B-RAF inhibitor SB-590885 was previously shown to inhibit ERK phosphorylation and to induce G_1 arrest in melanoma cells with wild-type *KRAS* (36, 37). In contrast, we found that depletion of C-RAF did not result in inhibition of ERK phosphorylation in NSCLC cells. ERK activation was previously shown to be conserved in cells derived from C-RAF knockout mice, suggesting that C-RAF is dispensable for ERK signaling (38, 39). Together, the present data suggest that B-RAF-ERK signaling, rather than C-RAF signaling, is a potential therapeutic target in NSCLC cells with wild-type *KRAS*.

We showed that ERK phosphorylation was not inhibited by sorafenib in two NSCLC cell lines (A549 and H460) harboring mutant *KRAS*, consistent with previous observations (16). We further showed this to be the case in two additional such cell lines (H358 and H23). Such results were previously suggested to be due to the existence of RAF-independent ERK activation in

NSCLC cells with mutant *KRAS* (16). However, we have now shown that B-RAF depletion resulted in inhibition of ERK activation in these cells. Our data therefore suggest that sorafenib is not able to attenuate the constitutive activation of the B-RAF-ERK pathway characteristic of NSCLC cells harboring mutant *KRAS* (40). Despite the sustained activation of B-RAF-ERK signaling in such cells, sorafenib inhibited cell proliferation and induced G_1 arrest in NSCLC cells with mutant *KRAS* as well as in those with wild-type *KRAS*. These data suggest that sorafenib targets a different pathway in its inhibitory effect on cell growth in NSCLC cells with mutant *KRAS*. Whereas sorafenib inhibits the kinase activity of both B-RAF and C-RAF, it shows a higher affinity for C-RAF (16). We found that depletion of C-RAF by RNA interference inhibited cell proliferation and induced G_1 arrest, without affecting ERK phosphorylation, in NSCLC cells with mutant *KRAS*, whereas it did not exhibit such effects in NSCLC cells harboring wild-type *KRAS*. Depletion of B-RAF also inhibited the growth of NSCLC cells with mutant *KRAS*, although this effect was not as pronounced as that in those with wild-type *KRAS*. These data indicate that NSCLC cells with mutant *KRAS* are dependent on C-RAF signaling to a greater extent than on B-RAF-ERK signaling for cell proliferation but that both pathways participate in regulation of the growth of these cells. Melanoma cells that have acquired resistance to a specific B-RAF inhibitor were recently shown to have switched their dependency from B-RAF to C-RAF (41). These observations suggest that RAF proteins are functionally interchangeable in the regulation of cell growth. Our data thus indicate that C-RAF signaling is a potential therapeutic target in NSCLC cells with mutant *KRAS*. RAF family proteins are also implicated in regulation of cell cycle progression in a manner independent of the ERK pathway (18, 38, 42, 43). C-RAF has been shown to exist in a complex with Cdc25, which activates the cyclin E-Cdk2 complex and promotes the G_1-S phase transition (44, 45). Cyclin E is thus postulated to be a downstream effector of C-RAF. In the present study, we found that either C-RAF depletion or sorafenib treatment induced G_1 arrest and down-regulation of cyclin E in NSCLC cells with mutant *KRAS*. Although we cannot exclude a possible role for other cell cycle

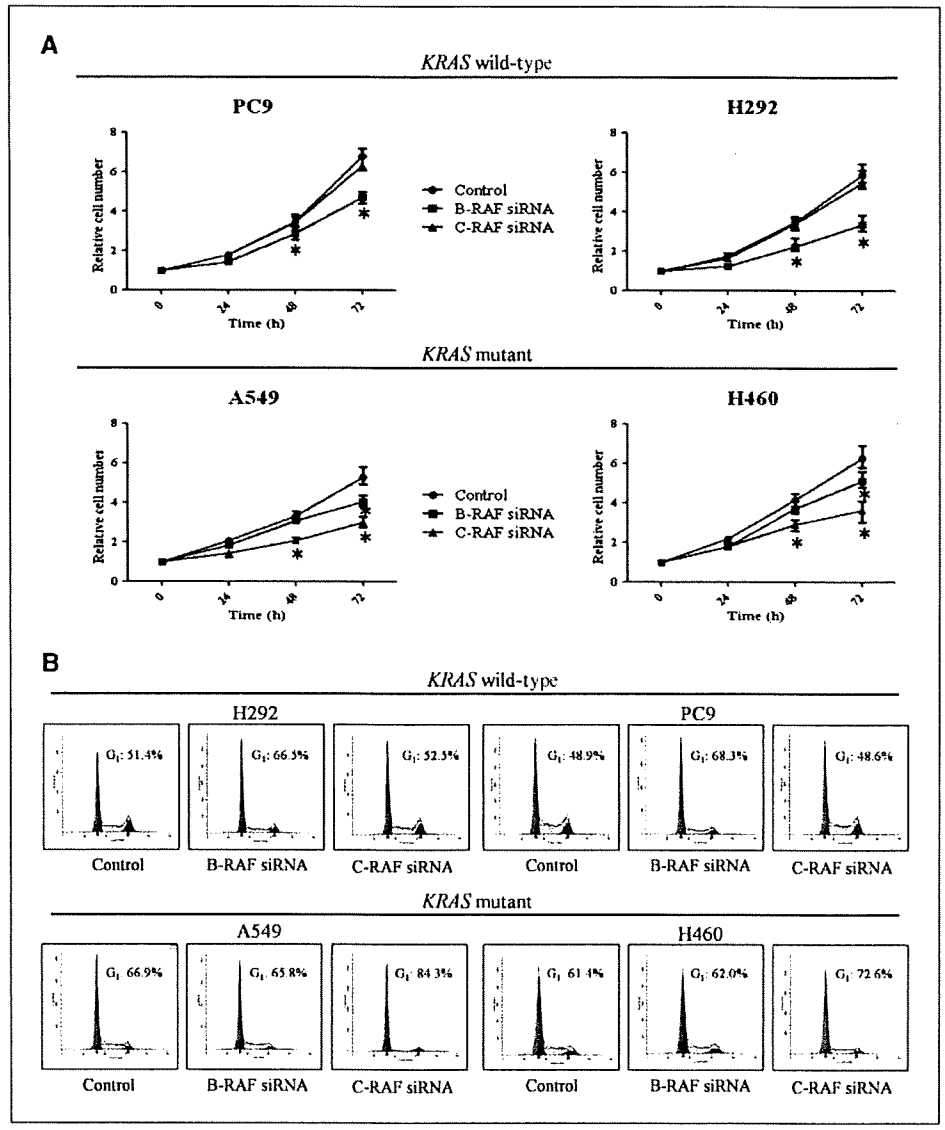

Figure 5. Effects of B-RAF or C-RAF depletion on cell proliferation and cell cycle distribution in NSCLC cells. *A*, cells harboring wild-type or mutant *KRAS* were transfected with nonspecific (control), B-RAF, or C-RAF siRNAs for the indicated times, after which the number of viable cells was determined by staining with trypan blue. The number of viable cells is expressed relative to the value for time 0. *Points*, mean values from three independent experiments; *bars*, SD. *, $P < 0.05$ versus the corresponding value for cells transfected with the nonspecific siRNA. *B*, cells were transfected as in *A* for 48 h, fixed, stained with propidium iodide, and analyzed for cell cycle distribution by flow cytometry. The percentage of cells in G_1 phase is indicated. Data are from representative experiments that were repeated on three separate occasions.

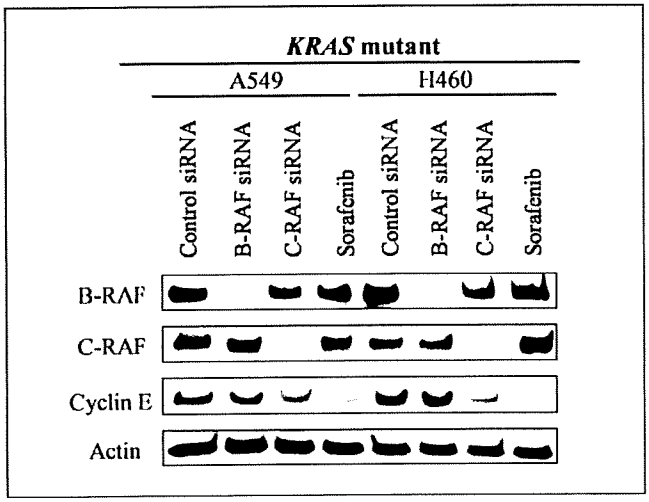

Figure 6. Effects of C-RAF depletion or sorafenib on cyclin E expression in NSCLC cells with mutant *KRAS*. Cells harboring mutant *KRAS* were transiently transfected for 48 h with nonspecific (control), B-RAF, or C-RAF siRNAs or were exposed to 15 μmol/L sorafenib for 24 h in complete medium. Cell lysates were then prepared and subjected to immunoblot analysis with antibodies to B-RAF, C-RAF, cyclin E, and β-actin.

proteins, our present data suggest that the observed down-regulation of cyclin E may contribute to the G_1 arrest induced by C-RAF depletion or by sorafenib in NSCLC cells with mutant *KRAS*.

Sorafenib inhibits several RTKs that participate in neovascularization, including vascular endothelial growth factor receptor (VEGFR)-2 and VEGFR-3 (16). Inhibition of angiogenesis might thus be expected to contribute to the inhibition of tumor growth by this drug in addition to its effects on RAF signaling. Although sorafenib was previously shown to inhibit the growth of a variety of human tumor xenografts in mice (13, 16, 46), it has been difficult to measure the relative contributions of its antiangiogenic activity and its direct antitumor activity mediated by RAF inhibition. In the present study, we have provided insight into the inhibitory effect of sorafenib on tumor cell growth *in vitro* that is mediated by inhibition of RAF signaling pathways. Our results suggest that sorafenib targets B-RAF in NSCLC cells with wild-type *KRAS* and C-RAF in those with mutant *KRAS*, and they provide a rationale for future clinical investigation of the therapeutic efficacy of sorafenib for NSCLC patients.

Disclosure of Potential Conflicts of Interest

No potential conflicts of interest were disclosed.

Acknowledgments

Received 3/23/09; revised 5/22/09; accepted 6/15/09; published OnlineFirst 7/28/09.

The costs of publication of this article were defrayed in part by the payment of page charges. This article must therefore be hereby marked *advertisement* in accordance with 18 U.S.C. Section 1734 solely to indicate this fact.

We thank H. Saya, K. Nishio, and T. Arao for helpful discussion.

References

1. Jemal A, Siegel R, Ward E, et al. Cancer statistics, 2008. CA Cancer J Clin 2008;58:71–96.
2. Eccles SA. Parallels in invasion and angiogenesis provide pivotal points for therapeutic intervention. Int J Dev Biol 2004;48:583–98.
3. Sridhar SS, Hedley D, Siu LL. Raf kinase as a target for anticancer therapeutics. Mol Cancer Ther 2005;4:677–85.
4. Adjei AA, Hillman SL. A front-line window of opportunity phase II study of sorafenib in patients with advanced non-small cell lung cancer: a North Central Cancer Treatment Group Study. Proc Am Soc Clin Oncol 2007;25:S18.
5. Gatzemeier U, Fosella F. Phase II trial of singe-agent sorafenib in patients with advanced non-small cell lung carcinoma. J Clin Oncol 2006;24:7002.
6. Gutierrez SKM, Allen D, Turkbey B, et al. A phase II study of multikinase inhibitor sorafenib in patients with relapsed non-small cell lung cancer [abstract 19084]. J Clin Oncol 2008;26:S712.
7. Schiller JH, Hanna NH, Traynor AM, Carbone DP. A randomized discontinuation phase II study of sorafenib versus placebo in patients with non-small cell lung cancer who have failed at least two prior chemotherapy regimens [abstract 8014]. J Clin Oncol 2008;26:S427.
8. Rodenhuis S, van de Wetering ML, Mooi WJ, Evers SG, van Zandwijk N, Bos JL. Mutational activation of the K-ras oncogene. A possible pathogenetic factor in adenocarcinoma of the lung. N Engl J Med 1987;317:929–35.
9. Garnett MJ, Marais R. Guilty as charged: B-RAF is a human oncogene. Cancer Cell 2004;6:313–9.
10. Panka DJ, Wang W, Atkins MB, Mier JW. The Raf inhibitor BAY 43-9006 (sorafenib) induces caspase-independent apoptosis in melanoma cells. Cancer Res 2006;66:1611–9.
11. Molhoek KR, Brautigan DL, Slingluff CL, Jr. Synergistic inhibition of human melanoma proliferation by combination treatment with B-Raf inhibitor BAY43-9006 and mTOR inhibitor rapamycin. J Transl Med 2005;3:39.
12. Lasithiotakis KG, Sinnberg TW, Schittek B, et al. Combined inhibition of MAPK and mTOR signaling inhibits growth, induces cell death, and abrogates invasive growth of melanoma cells. J Invest Dermatol 2008;128:2013–23.
13. Henderson YC, Ahn SH, Kang Y, Clayman GL. Sorafenib potently inhibits papillary thyroid carcinomas harboring RET/PTC1 rearrangement. Clin Cancer Res 2008;14:4908–14.
14. Smalley KS, Xiao M, Villanueva J, et al. CRAF inhibition induces apoptosis in melanoma cells with non-V600E BRAF mutations. Oncogene 2009;28:85–94.
15. Okabe T, Okamoto I, Tamura K, et al. Differential constitutive activation of the epidermal growth factor receptor in non-small cell lung cancer cells bearing EGFR gene mutation and amplification. Cancer Res 2007;67:2046–53.
16. Wilhelm SM, Carter C, Tang L, et al. BAY 43-9006 exhibits broad spectrum oral antitumor activity and targets the RAF/MEK/ERK pathway and receptor tyrosine kinases involved in tumor progression and angiogenesis. Cancer Res 2004;64:7099–109.
17. Strumberg D, Clark JW, Awada A, et al. Safety, pharmacokinetics, and preliminary antitumor activity of sorafenib: a review of four phase I trials in patients with advanced refractory solid tumors. Oncologist 2007;12:426–37.
18. Wojnowski L, Stancato LF, Larner AC, Rapp UR, Zimmer A. Overlapping and specific functions of Braf and Craf-1 proto-oncogenes during mouse embryogenesis. Mech Dev 2000;91:97–104.
19. Dobashi Y. Cell cycle regulation and its aberrations in human lung carcinoma. Pathol Int 2005;55:95–105.
20. Buttitta F, Barassi F, Fresu G, et al. Mutational analysis of the HER2 gene in lung tumors from Caucasian patients: mutations are mainly present in adenocarcinomas with bronchioloalveolar features. Int J Cancer 2006;119:2586–91.
21. Suzuki M, Shigematsu H, Iizasa T, et al. Exclusive mutation in epidermal growth factor receptor gene, HER-2, and KRAS, and synchronous methylation of nonsmall cell lung cancer. Cancer 2006;106:2200–7.
22. Graziano SL, Gamble GP, Newman NB, et al. Prognostic significance of K-ras codon 12 mutations in patients with resected stage I and II non-small-cell lung cancer. J Clin Oncol 1999;17:668–75.
23. Slebos RJ, Kibbelaar RE, Dalesio O, et al. K-ras oncogene activation as a prognostic marker in adenocarcinoma of the lung. N Engl J Med 1990;323:561–5.
24. Winton T, Livingston R, Johnson D, et al. Vinorelbine plus cisplatin vs. observation in resected non-small-cell lung cancer. N Engl J Med 2005;352:2589–97.
25. Pao W, Wang TY, Riely GJ, et al. KRAS mutations and primary resistance of lung adenocarcinomas to gefitinib or erlotinib. PLoS Med 2005;2:e17.
26. Massarelli E, Varella-Garcia M, Tang X, et al. KRAS mutation is an important predictor of resistance to therapy with epidermal growth factor receptor tyrosine kinase inhibitors in non-small-cell lung cancer. Clin Cancer Res 2007;13:2890–6.
27. Marks JL, Broderick S, Zhou Q, et al. Prognostic and therapeutic implications of EGFR and KRAS mutations in resected lung adenocarcinoma. J Thorac Oncol 2008;3:111–6.
28. Baselga J, Rosen N. Determinants of RASistance to anti-epidermal growth factor receptor agents. J Clin Oncol 2008;26:1582–4.
29. Hao H, Muniz-Medina VM, Mehta H, et al. Context-dependent roles of mutant B-Raf signaling in melanoma and colorectal carcinoma cell growth. Mol Cancer Ther 2007;6:2220–9.
30. Jane EP, Premkumar DR, Pollack IF. Coadministration of sorafenib with rottlerin potently inhibits cell proliferation and migration in human malignant glioma cells. J Pharmacol Exp Ther 2006;319:1070–80.
31. Ambrosini G, Cheema HS, Seelman S, et al. Sorafenib inhibits growth and mitogen-activated protein kinase signaling in malignant peripheral nerve sheath cells. Mol Cancer Ther 2008;7:890–6.
32. Villanueva J, Yung Y, Walker JL, Assoian RK. ERK activity and G_1 phase progression: identifying dispensable versus essential activities and primary versus secondary targets. Mol Biol Cell 2007;18:1457–63.

33. Jones SM, Kazlauskas A. Growth-factor-dependent mitogenesis requires two distinct phases of signalling. Nat Cell Biol 2001;3:165–72.
34. Yamamoto T, Ebisuya M, Ashida F, Okamoto K, Yonehara S, Nishida E. Continuous ERK activation downregulates antiproliferative genes throughout G_1 phase to allow cell-cycle progression. Curr Biol 2006;16:1171–82.
35. Fassett JT, Tobolt D, Nelsen CJ, Albrecht JH, Hansen LK. The role of collagen structure in mitogen stimulation of ERK, cyclin D1 expression, and G_1-S progression in rat hepatocytes. J Biol Chem 2003;278:31691–700.
36. Smalley KS, Lioni M, Dalla Palma M, et al. Increased cyclin D1 expression can mediate BRAF inhibitor resistance in BRAF V600E-mutated melanomas. Mol Cancer Ther 2008;7:2876–83.
37. King AJ, Patrick DR, Batorsky RS, et al. Demonstration of a genetic therapeutic index for tumors expressing oncogenic BRAF by the kinase inhibitor SB-590885. Cancer Res 2006;66:11100–5.
38. Huser M, Luckett J, Chiloeches A, et al. MEK kinase activity is not necessary for Raf-1 function. EMBO J 2001;20:1940–51.
39. Mikula M, Schreiber M, Husak Z, et al. Embryonic lethality and fetal liver apoptosis in mice lacking the c-raf-1 gene. EMBO J 2001;20:1952–62.
40. Salgia R, Skarin AT. Molecular abnormalities in lung cancer. J Clin Oncol 1998;16:1207–17.
41. Montagut C, Sharma SV, Shioda T, et al. Elevated CRAF as a potential mechanism of acquired resistance to BRAF inhibition in melanoma. Cancer Res 2008;68:4853–61.
42. Baumann B, Weber CK, Troppmair J, et al. Raf induces NF-κB by membrane shuttle kinase MEKK1, a signaling pathway critical for transformation. Proc Natl Acad Sci U S A 2000;97:4615–20.
43. Galaktionov K, Jessus C, Beach D. Raf1 interaction with Cdc25 phosphatase ties mitogenic signal transduction to cell cycle activation. Genes Dev 1995;9:1046–58.
44. Kerkhoff E, Rapp UR. Cell cycle targets of Ras/Raf signalling. Oncogene 1998;17:1457–62.
45. Hindley A, Kolch W. Extracellular signal regulated kinase (ERK)/mitogen activated protein kinase (MAPK)-independent functions of Raf kinases. J Cell Sci 2002;115:1575–81.
46. Liu L, Cao Y, Chen C, et al. Sorafenib blocks the RAF/MEK/ERK pathway, inhibits tumor angiogenesis, and induces tumor cell apoptosis in hepatocellular carcinoma model PLC/PRF/5. Cancer Res 2006;66:11851–8.

Cancer Science
The official journal of the Japanese Cancer Association JCA

Effects of Src inhibitors on cell growth and epidermal growth factor receptor and MET signaling in gefitinib-resistant non-small cell lung cancer cells with acquired *MET* amplification

Takeshi Yoshida,[1] Isamu Okamoto,[1,6] Wataru Okamoto,[1] Erina Hatashita,[1] Yuki Yamada,[1] Kiyoko Kuwata,[1] Kazuto Nishio,[2] Masahiro Fukuoka,[3] Pasi A. Jänne[4,5] and Kazuhiko Nakagawa[1]

[1]Department of Medical Oncology, Kinki University School of Medicine, Osaka-Sayama, Osaka; [2]Department of Genome Biology, Kinki University School of Medicine, Osaka-Sayama, Osaka; [3]Department of Medical Oncology, Kinki University School of Medicine, Sakai Hospital, Minami-ku Sakai, Osaka, Japan; [4]Lowe Center for Thoracic Oncology, Dana-Farber Cancer Institute, Boston; [5]Department of Medical Oncology, Dana-Farber Cancer Institute, Boston, MA, USA

(Received August 9, 2009/Revised September 6, 2009/Accepted September 7, 2009)

The efficacy of epidermal growth factor receptor (EGFR)–tyrosine kinase inhibitors such as gefitinib and erlotinib in non-small cell lung cancer (NSCLC) is often limited by the emergence of drug resistance conferred either by a secondary T790M mutation of *EGFR* or by acquired amplification of the *MET* gene. We now show that the extent of activation of the tyrosine kinase Src is markedly increased in gefitinib-resistant NSCLC (HCC827 GR) cells with *MET* amplification compared with that in the gefitinib-sensitive parental (HCC827) cells. In contrast, the extent of Src activation did not differ between gefitinib-resistant NSCLC (PC9/ZD) cells harboring the T790M mutation of *EGFR* and the corresponding gefitinib-sensitive parental (PC9) cells. This activation of Src in HCC827 GR cells was largely abolished by the MET-TKI PHA-665752 but was only partially inhibited by gefitinib, suggesting that Src activation is more dependent on MET signaling than on EGFR signaling in gefitinib-resistant NSCLC cells with *MET* amplification. Src inhibitors blocked Akt and Erk signaling pathways, resulting in both suppression of cell growth and induction of apoptosis, in HCC827 GR cells as effectively as did the combination of gefitinib and PHA-665752. Furthermore, Src inhibitor dasatinib inhibited tumor growth in HCC827 GR xenografts to a significantly greater extent than did treatment with gefitinib alone. These results provide a rationale for clinical targeting of Src in gefitinib-resistant NSCLC with *MET* amplification. (*Cancer Sci* 2009)

Upregulation of the EGFR occurs frequently and is negatively correlated with prognosis in many types of human malignancy.[1,2] Recognition of the role of EGFR in carcinogenesis has prompted the development of EGFR-targeted therapies.[3] TKI of EGFR, such as gefitinib and erlotinib, both of which compete with ATP for binding to the tyrosine kinase pocket of the receptor, have been extensively studied in patients with NSCLC.[4] Sensitivity to these drugs has been correlated with the presence of somatic mutations that affect the kinase domain of EGFR, such as deletions in exon 19 and the L858R mutation in exon 21 of the *EGFR* gene.[5–15] However, the acquisition of an additional mutation (T790M) in exon 20 of *EGFR* results in the development of resistance to EGFR-TKI.[16–19] Irreversible EGFR-TKI are thought to be a potential therapeutic option for overcoming such resistance.[20,21] Amplification of the gene for the receptor tyrosine kinase MET has also recently been identified as a mechanism of gefitinib resistance, being detected in 22% of tumor samples from NSCLC patients with *EGFR* mutations who acquired gefitinib resistance.[22,23] Exposure of gefitinib-resistant NSCLC cells with *MET* amplification to the MET-TKI PHA-665752 or to gefitinib alone did not inhibit cell growth or survival signaling, given that both EGFR and MET signaling were found to be activated and to be mediated by ErbB3 (also known as Her3) in these cells.[22,23] However, the combination of gefitinib and PHA-665752 overcame gefitinib resistance attributable to *MET* amplification.[22,23] No single agent that overcomes such resistance has been identified to date.

The proto-oncogene *SRC* has been implicated in the development and poor clinical prognosis of several types of solid tumor as a result of the mediation by its product of signaling between integrins or receptor tyrosine kinases and their downstream effectors.[24–26] We have examined the potential role of Src in EGFR or MET signaling and whether Src inhibitors might block these signaling pathways in gefitinib-resistant NSCLC cells with *MET* amplification. We also evaluated the potential antitumor effect of Src inhibitors in order to provide insight into the mechanism by which such inhibitors might overcome gefitinib resistance in NSCLC cells with *MET* amplification.

Materials and Methods

Cell lines and reagents. The human NSCLC cell lines H1299, H460, HCC827, HCC827 GR5, HCC827 GR6, and PC9 were obtained as described previously.[22,27] H1838 and H820 cells were obtained from the American Type Culture Collection (Manassas, VA, USA). EBC-1 cells were obtained from the Health Science Research Resources Bank (Tokyo, Japan). PC9/ZD cells were established as a gefitinib-resistant clone from PC9 cells as previously described[28] and were shown to harbor the T790M mutation of *EGFR* by both PCR invader and PCR clamp assays carried out as previously described.[29,30] HCC827, PC9, and PC9/ZD cells were cultured under a humidified atmosphere of 5% CO_2 at 37°C in RPMI-1640 medium (Sigma, St Louis, MO, USA) supplemented with 10% FBS. HCC827 GR5 and HCC827 GR6 cells were cultured in RPMI-1640 medium supplemented with 10% FBS and 1 μM gefitinib. Dasatinib was kindly provided by Bristol-Myers Squibb (New York, NY, USA), gefitinib was obtained from AstraZeneca (Macclesfield, UK), PP1 was from Biomol Research Laboratories (Plymouth Meeting, PA, USA), and PHA-665752 was from Tocris Bioscience (Bristol, UK).

[6]To whom correspondence should be addressed.
E-mail: chi-okamoto@dotd.med.kindai.ac.jp

doi: 10.1111/j.1349-7006.2009.01368.x

Immunoblot analysis. Immunoblot analysis was carried out as described previously.[27] Antibodies to the Y845-phosphorylated form of EGFR, to EGFR, to phosphorylated Erk, to Erk, to phosphorylated Akt, to Akt, and to β-actin as well as HRP-conjugated goat antibodies to mouse or rabbit IgG were obtained as described previously.[27] Antibodies to the Y1234/Y1235-phosphorylated form of MET, to the Y1289-phosphorylated form of ErbB3, to the Y416-phosphorylated form of Src, to Src, and to PARP were obtained from Cell Signaling Technology (Beverly, MA, USA). Antibodies to MET were from Zymed (South San Francisco, CA, USA) and those to ErbB3 were from Santa Cruz Biotechnology (Santa Cruz, CA, USA).

Immunoprecipitation assay. Total cell lysates (500 μg protein) were incubated overnight at 4°C with 5 μg of a mouse monoclonal antibody (H-12) to total Src (Santa Cruz Biotechnology) in a final volume of 200 μL. The immune complexes were precipitated by further incubation for 2 h at 4°C with a suspension of protein G- and protein A-conjugated agarose (Calbiochem, Darmstadt, Germany). The immunoprecipitates were resolved by SDS-PAGE on a 7.5% gel, and the separated proteins were subjected to immunoblot analysis as described previously,[27] with the exception that the incubation with primary antibodies was carried out for 48 h.

Cell growth inhibition assay. Cells were plated in 96-well flat-bottomed plates and cultured for 24 h before exposure to various concentrations of tested drugs for 72 h. TetraColor One (5 mM tetrazolium monosodium salt and 0.2 mM 1-methoxy-5-methyl phenazinium methylsulfate; Seikagaku, Tokyo, Japan) was then added to each well, and the cells were incubated for 3 h at 37°C before measurement of absorbance at 490 nm with a Multiskan Spectrum instrument (Thermo Labsystems, Boston, MA, USA). Absorbance values were expressed as a percentage of that for untreated cells.

Assessment of tumor growth inhibition *in vivo*. Tumor cells (2×10^6) were injected s.c. into the right hind leg of 7-week-old female athymic nude mice. The mice were divided into three treatment groups of five animals: those treated over 28 days by oral gavage daily of vehicle, gefitinib (50 mg/kg), or dasatinib (15 mg/kg). Treatment was initiated when tumors in each group achieved an average volume of 200 mm^3, with tumor volume being determined twice weekly after the onset of treatment from caliper measurement of tumor length (L) and width (W) according to the formula $LW^2/2$.

Statistical analysis. Data are presented as means ± SE as indicated and were analyzed by Student's t-test. A P-value of <0.05 was considered statistically significant.

Results

Src is activated in gefitinib-resistant NSCLC cells with *MET* amplification. Amplification of *MET* is one mechanism for the acquisition of resistance to EGFR-TKI in NSCLC.[22,23] To explore approaches that might overcome such resistance, we examined the activation status of several signaling molecules in sublines of the gefitinib-sensitive, *EGFR* mutation-positive human NSCLC cell line HCC827 that have acquired *MET* amplification and gefitinib resistance. Immunoblot analysis revealed that the level of phosphorylation (activation) of both MET and ErbB3 was markedly increased in the HCC827 GR5 and GR6 sublines compared with the parental HCC827 cells (Fig. 1A), consistent with previous observations.[22,23] Furthermore, we found that the level of Src activation was also markedly increased in HCC827 GR cells compared with HCC827 cells (Fig. 1A). Such Src activation was not observed in PC9/ZD cells (Fig. 1A), a subline of the gefitinib-sensitive, *EGFR* mutation-positive human NSCLC cell line PC9 that has acquired a secondary T790M mutation of *EGFR* and consequent gefitinib resistance. These results thus suggested that Src might contribute to gefitinib resistance in NSCLC cells with *MET* amplification. We also found that H1838, EBC-1, and H820 NSCLC cells with *MET* amplification[31–33] have higher activation of Src than that in NSCLC cells without *MET* amplification (H1299 and H460) (Fig. 1B). These results suggested that Src activation is associated with *MET* amplification in NSCLC cells.

Src activation blocked by a MET inhibitor in gefitinib-resistant NSCLC cells with *MET* amplification. Src associates with many receptor tyrosine kinases including EGFR and MET and transduces signals to a variety of downstream effectors of these receptors.[24–26,34–36] To examine whether Src participates in MET or EGFR signaling in cells with *EGFR* mutations and with or without *MET* amplification, we examined the effects of the MET inhibitor PHA-665752 or the EGFR-TKI gefitinib on Src

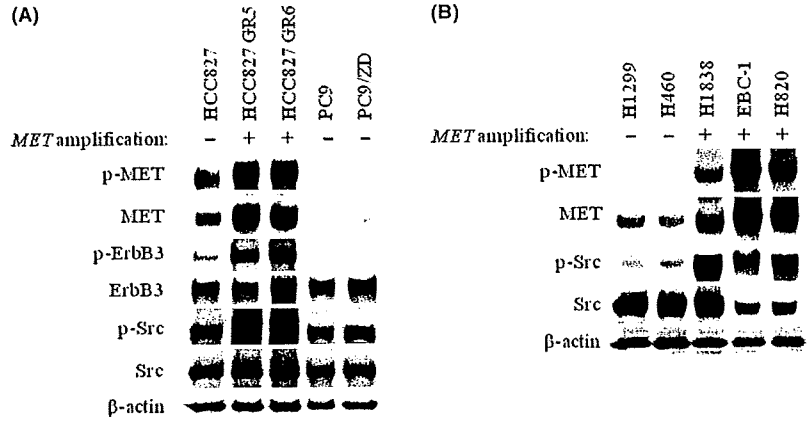

Fig. 1. Activation of Src in non-small cell lung cancer cells with or without *MET* amplification. (A) HCC827 cells, their gefitinib-resistant clones with *MET* amplification (HCC827 GR5 and GR6), PC9 cells, and their gefitinib-resistant clone with a secondary T790M mutation of epidermal growth factor receptor (PC9/ZD) were incubated for 24 h in medium containing 10% serum. Cell lysates were then prepared and subjected to immunoblot analysis with antibodies to phosphorylated (p-) or total forms of MET, ErbB3, and Src as well as with those to β-actin (loading control). (B) H1299 and H460 cells without *MET* amplification, and H1838, EBC-1, and H820 cells with *MET* amplification were incubated for 24 h in medium containing 10% serum. Cell lysates were then prepared and subjected to immunoblot analysis with antibodies to phosphorylated (p-) or total forms of MET and Src as well as with those to β-actin (loading control).

doi: 10.1111/j.1349-7006.2009.01368.x

activation in HCC827 and HCC827 GR cells. In the parental HCC827 cells, Src activity (phosphorylation) was reduced by PHA-665752 and was abolished by gefitinib (Fig. 2A). In contrast, Src activation was partially reduced by PHA-665752 and was inhibited to a much lesser extent by gefitinib in HCC827 GR5 cells (Fig. 2A). Combined treatment with gefitinib and PHA-665752 resulted in complete suppression of Src activation in both the parental and GR cells (Fig. 2A). These results suggested that Src activation is dependent on MET signaling to a greater extent than on EGFR signaling in gefitinib-resistant cells with *MET* amplification, whereas the opposite is the case for cells without *MET* amplification.

Effects of Src inhibitors on EGFR, ErbB3, and MET activation in gefitinib-resistant NSCLC cells with *MET* amplification. Src activates EGFR by phosphorylating the Y845 residue of the receptor,[37] and it also interacts with MET.[35] We therefore examined the effects of the Src inhibitors PP1 and dasatinib on EGFR, ErbB3, and MET activation. Both PP1 and dasatinib abolished EGFR activation and inhibited ErbB3 and MET activation in parental HCC827 cells (Fig. 2A). In contrast, these Src inhibitors did not suppress ErbB3 or MET activation and induced only partial inhibition of EGFR activation in HCC827 GR5 cells (Fig. 2A), suggesting that *MET* amplification affects the interactions of EGFR, ErbB3, and MET with Src.

Increased association between MET and Src in gefitinib-resistant NSCLC cells with *MET* amplification. We examined the effects of *MET* amplification on the physical association of Src with EGFR, MET, and ErbB3. Src was immunoprecipitated from both HCC827 and HCC827 GR5 cell lysates, and the resulting precipitates were subjected to immunoblot analysis with antibodies to EGFR, MET, ErbB3, or Src. The amount of MET associated with Src was greater for HCC827 GR5 cells than for HCC827 cells, whereas the amount of EGFR associated with Src was greater for HCC827 cells than for HCC827 GR5 cells (Fig. 2B). No association of ErbB3 with Src was apparent for either cell type. These results suggested that *MET* amplification results in an increase in the association between MET and Src, as well as a concomitant decrease in that between EGFR and Src, in HCC827 GR cells.

Src inhibitors block Akt and Erk signaling in gefitinib-resistant NSCLC cells with *MET* amplification. We next examined the effects of the Src inhibitors PP1 and dasatinib on Akt and Erk signaling pathways, both of which are activated by EGFR and MET. Both PP1 and dasatinib induced complete inhibition of Akt and Erk activation, as did gefitinib, in the parental HCC827 cells (Fig. 2A). Consistent with previous observations,[22,23] the combination of gefitinib and PHA-665752 inhibited Akt and Erk activation in HCC827 GR5 cells, whereas neither agent alone had such an effect (Fig. 2A). Both PP1 and dasatinib inhibited Akt and Erk activation to similar extents as the combination of gefitinib and PHA-665752 in HCC827 GR5 cells (Fig. 2A). A single agent (Src inhibitor) was thus sufficient to block Akt and Erk signaling, which is important for cell survival and proliferation, respectively, in gefitinib-resistant NSCLC cells with *MET* amplification.

Src inhibitor dasatinib suppresses growth of gefitinib-resistant NSCLC cells with *MET* amplification. The combination of gefitinib and PHA-665752 was recently shown to inhibit the growth of, and to induce apoptosis in, HCC827 GR cells with *MET* amplification, whereas neither agent alone had such an effect.[22,23] Given that we found that Src inhibitors block Akt and Erk signaling pathways as effectively as the combination of gefitinib and PHA-665752 in such cells, we examined whether dasatinib might overcome gefitinib resistance in HCC827 GR cells. In the parental HCC827 cells, both gefitinib and dasatinib as well as the combination of gefitinib and PHA-665752 effectively inhibited cell growth, but PHA-665752 alone had less inhibitory effect (Fig. 3A). Dasatinib inhibited cell growth in a concentration-dependent manner by the same marked extent as the combination of gefitinib and PHA-665752, even in HCC827 GR5 cells, whereas neither gefitinib nor PHA-665752 alone had a substantial effect (Fig. 3B). We also examined the effect of dasatinib on apoptosis as assessed on the basis of cleavage of the enzyme PARP in both HCC827 and HCC827 GR5 cells. Dasatinib (but not gefitinib) induced apoptosis in HCC827 GR5 cells to the same marked extent as did the combination of gefitinib and PHA-665752, whereas dasatinib and gefitinib each induced apoptosis in the parental HCC827 cells (Fig. 3C). These results suggested that Src inhibitors efficiently induce growth inhibition and apoptosis in gefitinib-resistant NSCLC cells with *MET* amplification.

Src inhibitor dasatinib inhibits tumor growth in gefitinib-resistant NSCLC xenografts with *MET* amplification. To determine whether the efficacy of dasatinib in gefitinib-resistant NSCLC cells with *MET* amplification observed *in vitro* might also be apparent *in vivo*, we examined the antitumor effects of dasatinib in nude mice with solid tumors formed by HCC827 GR5 cells injected into the right hind leg. Gefitinib (50 mg/kg)

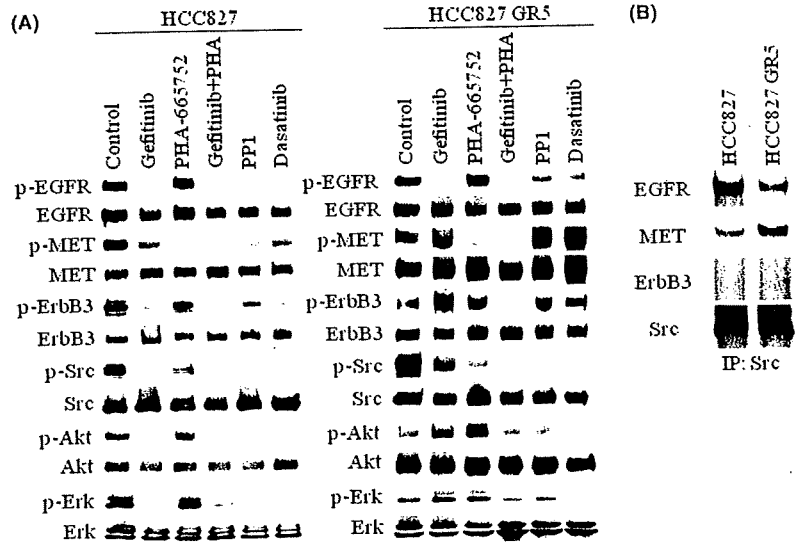

Fig. 2. Effects of various inhibitors on epidermal growth factor receptor (EGFR) and MET signaling in gefitinib-resistant non-small cell lung cancer cells with *MET* amplification. (A) HCC827 cells and a gefitinib-resistant clone with *MET* amplification (HCC827 GR5) were incubated for 12 h in the absence (control) or presence of gefitinib alone (1 μM), PHA-665752 alone (1 μM), gefitinib and PHA-665752 combined, PP1 (10 μM), or dasatinib (500 nM) in medium containing 10% serum. Cell lysates were then subjected to immunoblot analysis with antibodies to phosphorylated (p-) or total forms of EGFR, MET, ErbB3, Src, Akt, and Erk. (B) HCC827 and HCC827 GR5 cells were incubated for 24 h in medium containing 10% serum, lysed, and subjected to immunoprecipitation (IP) with an antibody to Src. The resulting precipitates were subjected to immunoblot analysis with antibodies to EGFR, MET, ErbB3, and Src.